Emerging trends in multiscale modeling of vascular pathophysiology: Organon-a-chip and 3D Printing

Karli Gold[1], **Akhilesh K. Gaharwar**[1,2,3,*], and **Abhishek Jain**[1,*]

[1]Department of Biomedical Engineering, Texas A&M University, College Station, TX 77843, USA

[2]Department of Material Sciences, Texas A&M University, College Station, TX 77843, USA

[3]Center for Remote Health and Technologies and Systems, Texas A&M University, College Station, TX 77843, USA

Abstract

Most biomedical and pharmaceutical research of the human vascular system aims to unravel the complex mechanisms which drive disease progression from molecular to organ levels. The knowledge gained can then be used to innovate diagnostic and treatment strategies that can ultimately be determined precisely for patients. Despite major advancements, current modeling strategies are often limited at identifying, quantifying, and dissecting specific cellular and molecular targets that regulate human vascular diseases. Therefore, development of multiscale modeling approaches is needed that can advance our knowledge and facilitate the design of nextgeneration therapeutic approaches in vascular diseases. This article critically reviews animal models, static *in vitro* systems, and dynamic *in vitro* culture systems currently used to model vascular diseases. A leading emphasis on the potential of emerging approaches, specifically organon-a-chip and three-dimensional (3D) printing, to recapitulate the innate human vascular physiology and anatomy is described. The applications of these approaches and future outlook in designing and screening novel therapeutics is also presented.

Keywords

Vascular disease; 3D printing; organ-on-a-chip; tissue modeling

1. INTRODUCTION

Vascular diseases, such as atherosclerosis, aneurysms, peripheral artery disease, and thrombosis, are the leading cause of morbidity and mortality worldwide, accounting for over 17 million deaths per year [1]. Despite major advancements to develop therapeutic interventions and treat vascular diseases, the pathophysiology as it applies to humans is still

Corresponding Author: *Abhishek Jain*, a.jain@tamu.edu; *Akhilesh K. Gaharwar*, gaharwar@tamu.edu, 101 Bizzell Street, ETB 5045, College Station, TX 77843, Phone: 979-845-5532, Fax: 979-845-4450.

largely unclear and treatments limited. If the status quo remains, the number of deaths are projected to reach epidemic proportions by 2030 (>23.6 million)[1]. Thus, there is crucial need to increase our understanding of vascular disease pathophysiology and assess emerging interventions to accelerate therapeutic development.

In order to model pathophysiology and the influence of various factors (e.g. drug, toxins, biological agents) on vasculature, animal models and cell culture techniques are the current gold standard. The aim of all these systems is to recapitulate the biological functions from the subcellular level to whole organs and have contributed immensely to our current understanding of vascular diseases and potential treatments. However, they do not adequately mimic human *in vivo* microenvironment at these multilevel scales (**Fig. 1A**). Moreover, these systems do not permit dissectible analysis of cell signaling mechanisms, therefore limiting their translational potential. Consequently, there is an unmet need to introduce a more predictable vascular disease model. In order to accomplish this, modeling approaches that evaluate molecular, cellular, tissue, and organ level variables are required for a systematic and robust assessment of mechanisms and therapeutic interventions in the blood vessel.

In this review, our focus is on the recent advances in multiscale modeling of vascular pathophysiology. First, the need for modeling pathophysiology of healthy and diseased vascular tissues will be briefly discussed, followed by a critical evaluation of animal models and *in vitro* culture systems. Then we will discuss the potential of organs-on-a-chip and three-dimensional (3D) printing as more predictive modalities, each having distinct positive features but also limitations. For example, the organ-on-a-chip technology is able to form tissue-tissue interfaces and combine physiological flow conditions in a variety of disease and organ models. However, these systems often contain a rectangular cross-sectional area, compared to round organs such as blood vessels. Alternatively, 3D printing can produce anatomically accurate vascular anatomy, including bifurcations and curvatures of vascular networks. However, 3D printed constructs are often difficult to integrate optical microscopy, as they cannot be miniaturized to micron sizes. Nevertheless, the unique aspects of organs-on-a-chip and 3D printing techniques are making them increasingly popular tools to understand the pathophysiology and function of patientspecific vascular diseases **(Fig. 1B)**. This is supported by the number of publications pertaining to organ-on-a-chip and 3D printing vascular disease models, undergoing an exponential increase over time (according to ISI Web of Science, July 2018, **Fig. 1C)**. Due to recent advances in the field of biomaterials, microfabrication, and additive manufacturing, we predict that these emerging *in vitro* vascular disease models will advance basic science and serve as a translational platform to design novel therapeutics and repurpose existing drugs.

2. NEED FOR MODELING VASCULAR SYSTEM AND PATHOPHYSIOLOGY

The vascular system is the largest organ system in the body and controls the transport of fluid to and from tissues. The vessels within the circulatory system form a multilayered architecture composed of endothelial cells (ECs), smooth muscle cells (SMCs), fibroblasts, and extracellular matrix (ECM). The innermost, or intima layer, contains a confluent layer of ECs that align with the direction of fluid flow. This layer serves as an active, selectively

permeable barrier between the vessel wall and circulating fluids [2]. The tunica media, or middle layer, is predominately composed of SMCs arranged circumferentially around the intima layer, providing structural stability and contractility to control blood flow [2, 3]. SMCs deposit collagen bundles around interconnected layered elastin networks, accounting for a majority of arterial mechanical properties[4]. The combination of elastin and collagen provide non-linear elasticity to vessel [5, 6]. The outer layer, or adventitia, of blood vessels is composed of fibroblasts and loose connective tissue, serving as an anchor for the vessel [7]. Together, this lamellar structure maintains several biological functions of the blood vessel, such as regulation, extravasation, or intravasation [8].

Vascular diseases result from changes in both structure and function of the blood vessel. For example, arteries may undergo structural changes due to degenerative conditions, infection, or inflammation causing disturbed blood flow [9]. This compromised flow results in an activated endothelium (**Fig. 2**) [10]. For example in atherosclerosis, once the endothelium becomes activated, it recruits monocytes and leukocytes, and secretes inflammatory chemokines [11]. Prothrombotic mediators are also released, encouraging platelet activation and SMC proliferation [11, 12]. Overall, these functional changes initiate geometrical modifications to the vessel, growing lesions that radially push towards the lumen, decreasing the vascular diameter and causing arterial hardening [6, 9, 10], and recruiting collagen fibers within the medial layer to support the vessel wall [13, 14]. Therefore, the dynamic complexity associated with human vascular diseases, specifically the vascular wall, is extremely difficult to fully recapitulate. However, vascular disease modeling is essential to progress our understanding of disease progression and ultimately, find immediate interventions. A predictable and translatable model includes the cross-talk between essential cellular and tissue components, specifically ECs, SMCs, ECM, and blood constituents under flow. The components needed and model used sets the stage for the biological problem to be solved.

3. ANIMAL MODELS

Animal models have been extensively used in the development of our current understanding of vascular diseases and treatment strategies. A major advantage of these systems is that they are able to provide integrated, multi-organ responses to a diverse range of experimental variables (for example, environmental factors, diet, drugs and toxins). Specifically, these models contain multi-cellular and dynamic tissue environments, thus eliciting a wholebody response that can be measured and predicted up to the pre-clinical stage of scientific discovery. For example, animal models have contributed immensely in the discovery of lipidbinding proteins, lipid-transfer proteins, cholesterol transporters, and enzymatic pathways in vascular disease genesis and progression [15, 16]. The mechanistic insight gained from animal models has aided in the development of interventions such as, tissue plasminogen activator to eliminate blood clots, several antiplatelet/anticoagulants to reduce the likelihood of blood clot formation, and ion-channel blockers to regulate muscle contraction/arrhythmias [17–19].

While several animal species are utilized, rodent vascular disease models are most frequently used due to ease of genetic manipulation, breeding, maintenance, cost, and time

frame [20, 21]. Contemporary molecular and genetic manipulations, such as the creation of hypercholesterolemia apolipoprotein E gene and low-density lipoprotein receptor knockout has humanized mouse models, thus enabling the study of inhibitors on vascular diseases and atherosclerosis with higher precision [19, 22]. Nevertheless, rodents exhibit several characteristics that differ from humans, limiting their ability to model human physiology and innate disease development. For example, lesion disruption and lipoprotein content is not identical between humans and mice [23]. Vessel sizes, blood composition, and biophysical properties exhibited by rodents can be vastly different from humans, thus providing poor predictive value to disease outcomes. Given such large discrepancies between these two species, large animal studies are often required even if rodent models are used.

Large animal models (i.e. porcine, rabbits, baboons, non-human primates), being closer in anatomy and genetic composition to humans, are used in advanced preclinical trials to model complex signaling pathways of vascular diseases and drug responses. The large size of these animals provides an increased tissue availability for histopathological analysis and facilitates non-invasive measurements, such as measuring vascular hemodynamics [24]. In addition, these models provide a more accurate representation of human metabolism and vascular anatomy (heart size and coronary circulation) [22]. Therefore, large animal models have thus far, predominately contributed to the drug discovery process in vascular diseases [23, 25]. However, large animals cannot easily undergo genetic modifications, thus their translational potential diminishes [26]. Furthermore, it is extremely difficult to dissect specific signaling pathways and analyze tissue-tissue or cell-cell interactions independent of other factors. To overcome the anatomical and physiological limitations of rodent and large animal models, non-human primates serve as ideal candidates who most closely reflect the innate biological processes within human vascular systems. Non-human primates (i.e. chimpanzees, baboons) are phylogenetically closest to humans, having analogous diet, metabolism, and development of vascular disease as they age [27–29]. However, use of non-human primates contain significant ethical restrictions and pose as a threat to maintaining biodiversity, therefore limiting their clinical practice [27].

In summary, animal models are able to provide full cellular compositions and complexity observed in human blood vessels, making them an indispensable tool in vascular disease modeling. However, the results obtained from animal models can be difficult to extrapolate, interpret, and do not always relate to human pathophysiology, limiting the translation potential of these models (**Table 1**). As a result, bioengineered *in vitro* approaches containing human-derived living cells within relevant microenvironments complement animal models and perhaps, even remove their need in the future.

4. *IN VITRO* MODELS

While animal models provide a top-down modeling approach, *in vitro* models offer a bottomup approach to model complex pathophysiology of vascular disease [30]. As a result, *in vitro* models allow the examination of specific cellular and molecular signaling events under defined chemical and mechanical conditions, thus making them an easily tunable system with reduced complexity. *In vitro* models can be static cultures of cells or include complex dynamic motions mimicking the *in vivo* environment more closely. However, both

these approaches have advantages and limitations, specifically depending upon the purpose of application.

4.1   STATIC *IN VITRO* CULTURE SYSTEMS

Since endothelial cells (ECs) line the walls of all blood vessels in circulation and are central to vascular function, most *in vitro* models analyze vascular diseases with EC monolayers [31–39]. Static well-plate systems with monoculture of ECs are simple to use and can be multiplexed. As a result, these systems have become the gold standard to understand endothelial biology [40], responses to internal or external environment changes [41–47], and for high throughput screening applications [17, 48].

Nevertheless, blood vessels are multicellular organs, containing external layers of SMCs, fibroblasts, components of epithelial cells, and embedded ECM. Several cadherin and integrin interactions occur within this lamellar structure that regulate cell behavior [7, 17, 49–52]. For example, ECs within the intima layer interacts with SMCs in the media layer. This interaction controls the upregulation of inflammatory cytokine expression (i.e. interleukin-8, IL-8, and monocyte chemotactic protein-1, MCP-1) and platelet-derived growth factor (PDGF), while inhibiting collagen and fibroblasts growth factor [50]. These cell-cell and cell-ECM interactions are critical for maintenance of proper blood vessel function. In order to achieve these EC-SMC cadherin interactions, various static co-culture systems have been utilized [48, 53–55]. Coculturing ECs and SMCs have shown mutual physical interactions which impact cell morphology, proliferation rate, and protein synthesis through the excretion of diffusible mediators [48, 53, 55]. Despite frequent use, monoculture or co-culture well-plate systems cannot recapitulate the complex, dynamic intercellular and organ-level signaling experienced by blood vessels. This is mainly due to changes from a natural 3D tissue environment to a 2D tissue culture, where the cells become exposed to a significantly altered microenvironment (e.g. surface stiffness, biochemical composition, local cell density) [56]. As a result, these static systems can also alter cell phenotype thus reducing the predictive power of these systems [14, 56]. For example, SMCs lose contractile proteins upon culture, rendering them incapable to modulate vascular tone [50]. Furthermore, static cultures cannot incorporate shear-dependent cell and tissue responses. For example, when the lumen is subjected to pulsatile blood flow, ECs respond through shear-sensitive ligands and integrins communicating with other regions of the vessel that respond to these signals. ECs respond to changes in shear by secreting or metabolizing vasoactive substances, such as nitric oxide and/or endothelin-1, inhibiting or exciting SMC growth, vasoconstriction, or vasodilation. These perturbations are impossible to mimic in 2D culture assays and therefore, flow-based culture systems are required to undertake such investigations.

4.2   DYNAMIC *IN VITRO* CULTURE SYSTEMS

In order to integrate mechanical forces to *in vitro* cell culture systems, parallel plate or twodimensional perfusion flow chambers have been used extensively [57, 58]. Traditional flow chambers are hollow conduits that provide a means to expose EC monolayers to fluidic forces on the millimeter scale, thus making it possible for the assessment of biophysical alterations involved in vascular disease [59–61]. However, due to the large volume of the

conduit, these techniques consume large amounts of medium, bioactive factors, and cells. Moreover, these macroscale devices do not represent the microphysiological environment of the smaller blood vessels, such as arterioles or capillaries. More recently, advances in microfabrication techniques have enabled rapid manufacturing of micron-scale flow chambers, termed microfluidic devices. These devices provide a reproducible and low-consumption platform to more precisely control biological conditions and the dynamic fluid environment relevant to arterial blood vessels and vascular diseases [62, 63]. A salient feature of microfluidic devices is that they allow quantitative assessment of hematological and microvascular processes of vascular disease. For example, a broad range of velocities that exists in the vascular system - ranging from 0.3 m/s in the aorta to 0.1 μm/s in vascular branches at the capillary level [64] can be applied within microfluidic devices, thus enabling assessment of the diverse shear-dependent signaling within the endothelium. In addition, flow perfusion provides a mechanism to continuously transport and distribute soluble factors, permitting long term culture of cells and providing a resource to model physical influences on cells (such as the rolling, decelerations, and arrests of blood-components with the endothelium) [65]. Overall, microfluidic methods have shown that they can be used to study whole-cell responses rather than individual mechano-receptors [66, 67]. A major advantage of this platform is that it can also include parenchymal cells and ECM, enabling for a method to model complex epithelial-endothelial-blood signaling that occurs in vascular disease, thus functioning as organs-on-a-chip or microphysiological systems.

5. EMERGING APPROACHES

From existing animal models and *in vitro* systems, a major hurdle in vascular science and the drug discovery process is the inability of these techniques to reliably predict the therapeutic targets and toxicities applicable to humans. As a result, major successes in pre-clinical trials have resulted in failures in human clinical trials. A key reason for this problem is that the current model systems do not recapitulate organ-level architecture and functions critical to the assessment of drugs, toxins and chemicals at a disease-and patient-specific level in humans. Therefore, there is a necessity for new disease models to emerge. With the advent of easy microfabrication methods, automated instrumentation, new biocompatible materials, stem cell differentiation to defined cell lineages, and molecular tools, microfluidic organ-on-a-chip devices and 3D printing have spurred new innovation and shown strong potential to address this unmet challenge. These emerging approaches to model vascular disease provides a unique solution by increasing the translational potential to humans and decreasing the mechanistic complexity associated with the experimental outputs. For example, microfluidic organ-on-a-chip devices can provide biological insight into pathophysiology by providing direct access via microscopy, biosensors, and genomic screening. In contrast, 3D printing can be used to fabricate a patient specific vascular disease model by recapitulating the structural and functional aspects of native tissues.

5.1 ORGAN-ON-A-CHIP

Recently, a new class of microfluidic devices known as organ-on-a-chip or microphysiological systems has emerged and shown to recapitulate 3D tissue architectures and physiological flow conditions in a variety of disease and organ models. These systems

have recreated the microenvironment of lung, liver, gut, kidney, skin, intestine and many other organs [56, 68–73], where cadherin interactions, tissue-tissue communication, and mechanical stimulation of fluids can be controlled in a physiologically-relevant manner not possible with animal models or classical *in vitro* systems. Organ-on-a-chip is broadly defined by the minimum amount of assembly of cells in a microenvironment that leads to mimicry of an organ-level function of a human. Importantly, this platform can include the endothelial lumen and blood flow in complex vascular geometries (such as, stenosis, aneurisms and bifurcations) and where the mechanical forces that govern endothelial activation can be included **(Fig. 3A)**. This inclusion offers enormous potential to model vascular disease mechanisms with higher specificity and accuracy not offered by conventional methods **(Table 2)**.

Recent studies have shown that atherothrombotic processes and platelet aggregation can be modeled with organ-on-a-chip platform [70, 74, 75]. In one such study, a microfluidic device containing a parallel array of stenosed microvessels was able to form platelet and fibrin-rich blood clots downstream of stenosis, as observed *in vivo* [72]. This device was then applied to predict anticoagulant and antiplatelet drug responses in patients on extracorporeal devices **(Fig. 3B)**. Another *in vitro* study applying a similar geometry validated that cell-secreted von Willebrand Factor (VWF) further exacerbates platelet recruitment and adhesion post-stenosis, like *in vivo* [31]. In another study, a microfluidic channel (vessel-on-a-chip) lined with living or chemically fixed human endothelium was demonstrated to maintain its ability to modulate hemostasis and thrombosis under arterial flow, thus serving as a potential diagnostic lab-on-achip device **(Fig. 3C)** [70, 76]. More recently, this vessel-on-a-chip system was able to predict toxicity of a drug compound that failed clinical trials but did not produce the same vascular sideeffects in primate studies [77]. Also, this organ-on-a-chip platform has provided more mechanistic understanding of vascular biology. For example, a recent work with microfluidic channels showed that proteins RhoA, Rac1, and N-cadherin regulate vascular permeability and barrier function [78]. Furthermore, immune cell interactions have also been assessed in these systems, demonstrating the role of inflammatory cells, such as neutrophils and T-cells, play on endothelium activation and consequent thrombosis formation [79–81].

More complex diseases, such as, cancer, infectious diseases and several genetic disorders, like sickle cell disease, result in vascular problems in patients and often, such patients encounter fatal strokes. Tissue and cell signaling in such diseases may constitute feedback between multiple organs and epithelial that regulate vascular function. For example, in cancer, the tumor cells release inflammatory factors that result in in vascular dysfunction [38]. Similarly, in pneumonia and other respiratory disorders, the alveolar epithelium may secrete factors that lead to platelet recruitment and thrombosis [39]. Organ-on-a-chip technology has been deployed to dissect tissue-tissue and drug-tissue interactions for systematic analysis of such complex vascular diseases. Recently, a model of lung thrombosis supported organ-level functional design by showing co-culture of human primary alveolar and endothelial lumen in adjacent microfluidic conduits, separated by thin layer of matrix [26]. When human whole blood was perfused through this lung thrombosis device, after introduction of lipopolysaccharide (LPS) in the abluminal epithelial compartment, thrombus

formed in the luminal compartment, as found identical to *in vivo* conditions. Further, an endothelium-specific therapeutic effect of an antithrombotic compound was identified with this system, which was not possible to be found using traditional animal models. These recent developments in vascular microphysiological systems are highly promising and provide major opportunities to visualize biological using microscopy, measured using biosensors, and quantified using analytical algorithms and genomic screening.

However, there are still some limitations in the current microfluidic designs that limit the extent to which vascular disease pathophysiology can be reconstructed. Virtually most published literature on organ-on-a-chip is based on the use of polydimethylsiloxane (PDMS) as the material of fabrication. The process of fabrication with PDMS, called soft lithography, is simple and adoptable to most lab environments. With soft lithography, multi-chamber microfluidic devices separated by thin film membranes to support tissue co-cultures can be designed with high fidelity. PDMS is also biocompatible, transparent, and permeable to gases, making it very suitable for cell culture. However, a major drawback of PDMS is that the material adsorbs small hydrophobic molecules, therefore making it very difficult to assess pharmacokinetics of drugs and toxins. For example, if the drug is absorbed by the PDMS, then its net concentration is lower, and potential therapeutic effect or toxicity might be underestimated. Thermoplastic materials are potential alternatives and have been used to make microfluidic chips, but they often auto-fluoresce during imaging, do not let oxygen diffuse through them making it harder for cells to survive for long durations, and can be very expensive for a high-throughput setting. Another potential limitation is that organ-on-a-chip models are subsets of the whole living organ. For example, the blood vessel-on-a-chip models published so far lack connective tissue, containing fibroblasts between the epithelium and endothelium, which may regulate vascular homeostasis and pathogenesis. In addition, pericytes or SMCs may need to be integrated under the endothelium for a complete biological output from these models. This is not necessarily a drawback because scientists can design the simplest model and then add additional complexity until the required combination is achieved for solving the problem of interest. For example, blood flow in arteries is pulsatile and will be a very interesting addition to vascular organ-on-achip technologies in the future. A major hurdle that still exists is that the cells used in these model systems may not always represent the phenotype of the local environment of the human disease or patient, and therefore, standardization of the cell-lines and growth protocols is necessary [30, 82, 83]. In addition, given the planar and thin (<1 mm in thickness) cellular arrangement, modeling drug-tissue interactions may be inaccurate and require careful scaling up due to varied drug pharmacokinetics and pharmacodynamics [35, 56, 84–87]. Also, organ-on-achip models may not always include the same cellular arrangements as *in vivo*. They are often designed as overlaying or side-by-side rectangular channels which make them unable to recapitulate the exact flow inside a cylindrical blood vessel. This may also alter endothelial function and affect the contractility-related mechanisms of cells. Finally, despite promising use of organ-on-a-chip, these models may not be appropriate to model the macroscale organ biology, for example, aorta or veins and therefore, different tools may be needed for such investigations.

5.2 3D PRINTING

Given that vascular diseases often originate in blood vessels with complex geometries, additive manufacturing, such as 3D printing (including 3D bioprinting), offers a vital tool to recapitulate a diseased anatomy. 3D printing is a fabrication technique used to mimic the anatomical complexity of native tissue, *via* a bottom-up approach, by depositing polymeric or cell-laden hydrogel based inks, in a layer-by-layer fashion **(Fig. 4A)** [88, 89]. The use of 3D printing to fabricate intricate geometries, such as bifurcations and curvatures, provides a comprehensive understanding and functional evaluation of patient-specific vascular disease symptoms [90, 91] **(Table 3)**. Recent advancements in 3D printing technology has resulted in the development of complex, anatomical structures, motivating its use in a variety of biomedical applications such as tissue modeling [92–94], pharmacological assessment of therapeutics (contractions of vascular wall in response to serotonin [95], endothelin-1 [95–97], prostaglandin $F_2\alpha$ [95], polyphenols from red wine [98, 99], and histamine [100]), and disease pathophysiology (neovascularization[101] EC permeability[102, 103], and hemodynamics[104, 105]).

A vital yet limiting component of the 3D printing design and implementation is the selection of materials, or bioinks. The materials used serve as an artificial ECM composed of natural, synthetic, or their combination to reproduce tissue microenvironments and permit for cellular functions observed on native ECM. Natural polymers encompass materials derived from natural sources, such as ECM constituents (e.g. collagen, elastin, and fibrin) or polysaccharidebased biomaterials (e.g. alginate, chitosan) [106–108]. These materials often contain celladhesive domains, driving for cell adhesion, migration, and proliferation. However, natural polymers often contain significant batch-to-batch variability, as well as a lack of control over the chemical and physical properties. To overcome the variability of natural polymers, synthetic polymers with desired chemical structures, mechanical integrity and functionality are used [109, 110]. However, synthetic materials lack biological recognition domains, resulting in limited cellmatrix interactions. In order to enhance or obtain bioactivity, synthetic polymers are modified with cell-responsive structures such as RGD-domains or natural polymers. Due to the inherent complexity of vascular tissue, combining both natural and synthetic polymers warrant for the fabrication of bioinks that can be finely tuned to obtain optimal material properties and enhanced bioactivity [111, 112]. The combination of both natural and synthetic polymers to fabricate vascular constructs enables for precise manipulations to model tissue compositions, architectures, and microenvironments in healthy and diseased conditions [113–115]. This permits for dissectible analysis of physiological changes that occurs with geometry, disease progression, and ageing [112, 116].

In order to further recapitulate ECM properties of vascular tissues, such as conductivity, nanomaterials such as carbon nanotubes [117, 118], graphene oxide [119], and gold nanorods [120] can be integrated into polymeric networks. These nanomaterials can also be used modify a materials printability to print anatomically scaled tissue structures that are able to model the macroscale organ biology. In a recent study, anatomically accurate bifurcating vascular constructs were 3D printed with precise geometries **(Fig. 4B)** [114, 121]. In this approach, bioink properties were optimized by controlling the interaction

between nanoparticles and polymeric network to obtain highly printable inks [113, 121–124]. Printability is a crucial property of bioinks that is defined by its ability to smoothly extrude into the intended architecture with high structural fidelity. These properties are governed by a materials rheological properties and crosslinking mechanisms [125]. Specifically, a bioink must first shear-thin, allowing for extrusion through a needle gauge, followed by rapid recoverability of the material's internal structure, permitting for shape retention into the deposited geometry [113]. A range of approaches have been developed to print custom scaffolds with enhanced fidelity, such as on-site curing of bioink[126, 127], printing into support bath[128–131], or exposing ions or temperature changes to retain a deposited shape [114, 121].

Aside from print fidelity, bioink selection is crucial as it can dictate cellular organization and functions. By modulating bioink properties, biophysical and biochemical microenvironments of human vascular diseases can be recapitulated [132]. For example, recent studies have utilized 3D printing to design a cardiac patch by mimicking the cardiac niche-like microenvironment in order to improve cardiomyocyte organization and maturity **(Fig. 4C)** [133, 134]. This 3D printed model was able to produce physiological responses to a androgen agonists (such as epinephrine; Epi - increases heartbeat frequency) and carbachol (CCH; decreases heartbeat frequency) [135]. In a similar study, 3D printing was used to fabricate constructs with specific surface topography to control cellular adhesion and alignment **(Fig. 4D)** [136, 137]. This approach is capable of mimicking some of the structural complexity observed with native vasculature. These proof-ofconcept studies highlight the versatility of 3D bioprinting to mimic structural and functional complexity of vascular tissues.

Although printing design has been used to dictate cellular arrangement on printed scaffolds, construct topography, stiffness, and architecture also strongly impact the model's predictability, specifically regarding the devices hemocompatibility. In healthy vasculature, blood does not clot due to a confluent layer of EC shielding the ECM from fluid contact fluid [138]. The ECs prevent clotting through the release of biochemical ques to the blood, such as heparans, thrombomodulin, tissue plasminogen activator, and adhesion proteins to dictate vascular function [139]. However, when the lumen is disrupted or damaged, the underlying ECM elicits highly thrombogenic properties, triggering immediate platelet adhesion and thrombosis [9, 140]. Bioink properties can be tuned to prevent this clotting cascade and improve upon the ink's hemocompatibility. Specifically, sub-micrometer rigids and grooves on the blood-contacting surface has been shown to decreases platelet adhesion and activation compared to smooth surfaces [141–143]. This is due to an increased surface area and geometrical constraints for platelet adhesion and activation. In addition, increased matrix stiffness (~ 5–50 kPa) has been shown to significantly enhance platelet adhesion and spreading, *via* Rac 1 and actomyosin activity [144–146]. Aside from surface roughness and matrix stiffness, other strategies, such as the inclusion thrombosis resistant materials [147, 148] or chemical modifications of the constructs surface [149, 150] greatly impact platelet interactions with the model.

3D printing can also be combined with other fabrication techniques, such as solution blow spinning, photolithography or self-assembly to imitate more complex structural features of

vascular tissues. For example, innate myocardium ECM consists of a well-organized, anisotropic tissue with conductive fibers [151, 152]. Electrospinning, an electrostatic fabrication technique to obtain micro- and nano-fibers, can be used to mimic structural organization of myocardium ECM by providing topological clue for cell alignment and impart directional properties. By combining electrospinning with 3D printing, a patient-specific vascular graft can be obtained **(Fig. 4E)**, which is difficult to obtained from either technique alone [153]. The topological clue provided by electrospun fibers facilitate formation of vascular tissue around the graft *in vivo* after 6 weeks. Interesting, the secreted ECM consists of predominantly collagen and elastin, which are similar to the native inferior vena cava. In addition, there was no observable calcification of the engineered graft [153]. This study indicated strong potential of combining 3D printing with other fabrication techniques such as electrospinning to mimic structural complexity of vascular anatomy. Aside from combining with other fabrication techniques, 3D printing has recently been used for a template micro molding technique **(Fig. 4F)** [76]. Complex vascular microchannels can be printed out of a sacrificial bioink, such as agarose [76], gelatin [154], or pluronics [106, 155, 156]. After the printed microchannels gel cooler temperatures, a cell-laden hydrogel precursor solution can be caster over the fibers and photo-crosslinked. Subsequently, the sacrificial microchannel templates are removed from the surrounding crosslinked hydrogel by increasing past the materials melting temperature. This fabrication technique enables the fabrication of anatomically accurate, perfusable microchannels and permit for co-culture of multiple cell types. The use of sacrificial material 3D printing provides a platform to create a fully perfusable microvascular network with different architectures and geometries.

Although 3D printed constructs are capable of mimicking the native structure of blood vessels and can model several aspects of vascular diseases, few significant hurdles still remain before this technology can be translated to preclinical trials or medical practice. Specifically, lack of bioinks that can truly mimic the mechanical and chemical properties of the ECM is a big limiting factor. For example, there is no bioink that can provides an accurate representation of abnormal features observed in vascular diseases, such as calcified structures, mechanical and chemical variations within tissues, or differences in mechanical properties of vascular structures during dynamic or static states [93]. Moreover, biological arrangement of cells and tissue observed *in vivo* is challenging to control *in vitro*. Although use of electrospinning and other microfabrication technology along with 3D printing can be used to provide some control over cellular arrangement, this relies on cells innate ability to self-organize. Overall, 3D printing is promising new approach to mimic human vascular pathophysiology and have strong potential to dissect tissue-tissue and drug-tissue interactions for systematic analysis of complex vascular diseases.

6.   FUTURE PROSPECTS AND CONCLUSION

Multiscale modeling of vascular pathophysiology can provide molecular and cellular insights to understand complex biochemical and biophysical mechanisms of the human vascular system. The current gold standard consists of animal *in vivo* models and *in vitro* cell culture, however significant limitations persists in both these approaches as they are not able to recapitulate human pathophysiology. Recent developments in fabrication techniques, such as organ-on-chip and 3D printing, provide a unique solution to mimic human vascular

function, thereby increasing the translational potential to humans and decreasing the mechanistic complexity associated with the experimental outputs. However, these emerging approaches are still in proof-of-concept stage and need further optimization to potentially aid in a better understanding of vascular pathophysiology while providing valuable tools for pharmaceutical research and translational outcomes. In order to utilize the full potential of organs-on-a-chip and 3D printing, as well as recapitulate critical aspects of vascular disease development and progression with high precision, the cell sources have to be primary and/or stem-cell derived. Human induced pluripotent stem cells (hiPSC) differentiated into targeted cell-lineages is an exciting new approach that may become the gold standard cell-source in these modeling systems in the future.

Similarly, the physical properties of biomaterials need to be optimized in term of composition, stiffness, anisotropy, and permeability, all which impact vascular pathophysiology and disease development (**Table 4**). In addition, the materials used to fabricate vascular tissues should be able to withstand long-term cell culture for the assessment of disease progression (e.g. from the observation of EC dysfunction to stenosis, and eventually a plaque rupture). Bioinks and scaffold materials that provide structure to organs-on-chips and 3D bioprinted tissues can be enhanced with nanoengineered particles to improve their mechanical and biochemical functionality. Also, currently available fabrication techniques produce constructs that are not able to form vasculature geometries with anatomical accuracy. Some printers, such as the nanobiological printers, are able to provide resolutions up to 5–20 μm, however it is not evident if these features can be translated to extrusion-based printers using biological relevant, cell-laden bioinks [125]. Considering these geometrical constraints, there is a need for a printer that is able to construct multi-material, hierarchical structures across multiple length scales to mimic native vasculature. This will enable for the fabrication of heterogeneous tissue consisting of adventitia, media, and intima layers, all comprised of different cell-laden bioinks [112, 157].

Given the increasing complexity of organ-on-a-chips and 3D printed structures, validation of the model to mimic *in vivo* conditions, such as cell phenotype and remodeling, are needed. Therefore, advanced imaging techniques, computational modeling, and the integration of genomics provide a means to further assess and validate engineered vascular models. Advanced imaging systems with enhanced penetration depth, such as optical coherence tomography (OCT) and photoacoustic tomography (PAT), would permit for visualization of the 3D structure and geometrical changes within the model. The use of more mature imaging modalities provides a means to non-invasively probe cell-cell and cell-matrix interactions when cultured within organon-a-chip devices and 3D printed models. In addition, emerging approaches also focus on the development of computational tools to model fluid dynamics, oxygen diffusion, cellular proliferation, remodeling, and viability within 3D models. This permits for researches to examine, assess, and optimize models prior to fabrication as well as correlate to *in vivo* observations. Furthermore, whole genome transcriptomic approaches can be applied to validate the cell behavior in response to materials to which they adhere to and to understand mechanistic pathways such that their function can be measured and designed for precision/personalized medicine[158].

In summary, the prospects of these emerging technologies are promising. The relationship between design, manufacturing, and assessment is closely related and never-ending, repeated cycle. Therefore, this process can be enhanced with bioengineering, material science, medicine, imaging, and genomic collaborations. Bringing these fields together will improve the success of these platforms to predict physiology and drug, toxin, and chemical responses at the patient level. **(Fig. 5)** [159]. As more progress is made in this direction, organs-on-a-chip and 3D bioprinting technologies are expected to add new knowledge to vascular disease pathophysiology and predict therapeutic responses and toxicities to drugs at a disease- and patient-specific level that is impossible with animal models, thus directly impacting the entire healthcare system

Acknowledgements

REFERENCES

[1]. Mozaffarian D, Benjamin EJ, Go AS, Arnett DK, Blaha MJ, Cushman M, de Ferranti S, Després J-P, Fullerton HJ, Howard VJ, Huffman MD, Judd SE, Kissela BM, Lackland DT, Lichtman JH, Lisabeth LD, Liu S, Mackey RH, Matchar DB, McGuire DK, Mohler ER, Moy CS, Muntner P, Mussolino ME, Nasir K, Neumar RW, Nichol G, Palaniappan L, Pandey DK, Reeves MJ, Rodriguez CJ, Sorlie PD, Stein J, Towfighi A, Turan TN, Virani SS, Willey JZ, Woo D, Yeh RW, Turner MB, Heart Disease and Stroke Statistics—2015 Update, A Report From the American Heart Association 131(4) (2015) e29–e322.

[2]. Wolf F, Vogt F, Schmitz-Rode T, Jockenhoevel S, Mela P, Bioengineered vascular constructs as living models for in vitro cardiovascular research, Drug Discovery Today 21(9) (2016) 1446–1455. [PubMed: 27126777]

[3]. Kinza Islam SBT, Nasser Rasha, Gater Deborah L, Pearson Tanthe E, Christoforoul N, and CM Teo Jeremy, Co-culture Methods Used to Model Atherosclerosis In Vitro Using Endothelial, Smooth Muscle and Monocyte Cells, SM Journal of Biomedical Engineering 2(1) (2016).

[4]. Huang AH, Balestrini JL, Udelsman BV, Zhou KC, Zhao L, Ferruzzi J, Starcher BC, Levene MJ, Humphrey JD, Niklason LE, Biaxial Stretch Improves Elastic Fiber Maturation, Collagen Arrangement, and Mechanical Properties in Engineered Arteries, Tissue Engineering Part C: Methods 22(6) (2016) 524–533. [PubMed: 27108525]

[5]. Claes E, Atienza JM, Guinea GV, Rojo FJ, Bernal JM, Revuelta JM, Elices M, Mechanical properties of human coronary arteries, 2010 Annual International Conference of the IEEE Engineering in Medicine and Biology, 2010, pp. 3792–3795.

[6]. Karimi A, Navidbakhsh M, Shojaei A, Faghihi S, Measurement of the uniaxial mechanical properties of healthy and atherosclerotic human coronary arteries, Materials Science and Engineering: C 33(5) (2013) 2550–2554. [PubMed: 23623067]

[7]. Gutterman DD, Adventitia-dependent influences on vascular function, American Journal of Physiology - Heart and Circulatory Physiology 277(4) (1999) H1265–H1272.

[8]. Segal SS, Cell-to-cell communication coordinates blood flow control, Hypertension 23(6 Pt 2) (1994) 1113–1120. [PubMed: 8206602]

[9]. Pathophysiology of Heart Disease: A collaborative Project of Medical Students and Faculty, Fourth ed., Lippincott Williams & Wilkins, Baltimore, MD, 2007.

[10]. Hansson Inflammation GK, Atherosclerosis, and Coronary Artery Disease, New England Journal of Medicine 352(16) (2005) 1685–1695. [PubMed: 15843671]

[11]. Hotamisligil GS, Endoplasmic reticulum stress and atherosclerosis, Nat Med 16(4) (2010) 396–399. [PubMed: 20376052]

[12]. Weber C, Noels H, Atherosclerosis: current pathogenesis and therapeutic options, Nat Med 17(11) (2011) 1410–1422. [PubMed: 22064431]

[13]. Wagenseil JE, Mecham RP, Vascular Extracellular Matrix and Arterial Mechanics, Physiological reviews 89(3) (2009) 957–989. [PubMed: 19584318]

[14]. Ryan AJ, Brougham CM, Garciarena CD, Kerrigan SW, O'Brien FJ, Towards 3D in vitro models for the study of cardiovascular tissues and disease, Drug Discovery Today 21(9) (2016) 1437–1445. [PubMed: 27117348]

[15]. Rosenson RS, Brewer HB, Jr, Barter PJ, Björkegren JLM, Chapman MJ, Gaudet D, Kim DS, Niesor E, Rye K-A, Sacks FM, Tardif J-C, Hegele RA, HDL and atherosclerotic cardiovascular disease: genetic insights into complex biology, Nature Reviews Cardiology 15 (2017) 9. [PubMed: 28795686]

[16]. Rye K-A, Barter PJ, Regulation of High-Density Lipoprotein Metabolism, Circulation Research 114(1) (2014) 143–156. [PubMed: 24385508]

[17]. Truskey GA, Endothelial Cell Vascular Smooth Muscle Cell Co-Culture Assay For High Throughput Screening Assays For Discovery of Anti-Angiogenesis Agents and Other Therapeutic Molecules, International journal of high throughput screening 2010(1) (2010) 171181.

[18]. Persidis A, Cardiovascular disease drug discovery, Nature Biotechnology 17 (1999) 930.

[19]. Gromo G, Mann J, Fitzgerald JD, Cardiovascular Drug Discovery: A Perspective from a Research-Based Pharmaceutical Company, Cold Spring Harbor Perspectives in Medicine 4(6) (2014).

[20]. Hampton T, How Useful Are Mouse Models for Understanding Human Atherosclerosis?, Review Examines the Available Evidence 135(18) (2017) 1757–1758.

[21]. von Scheidt M, Zhao Y, Kurt Z, Pan C, Zeng L, Yang X, Schunkert H, Lusis AJ, Applications and Limitations of Mouse Models for Understanding Human Atherosclerosis, Cell Metabolism 25(2) (2017) 248–261. [PubMed: 27916529]

[22]. Liao J, Huang W, Liu G, Animal models of coronary heart disease, Journal of Biomedical Research 31(1) (2017) 3–10.

[23]. Getz GS, Reardon CA, Animal Models of Atherosclerosis, Arteriosclerosis, Thrombosis, and Vascular Biology 32(5) (2012) 1104–1115.

[24]. Davies PF, Hemodynamic shear stress and the endothelium in cardiovascular pathophysiology, Nat Clin Pract Cardiovasc Med 6(1) (2009) 16–26. [PubMed: 19029993]

[25]. Emini Veseli B, Perrotta P, De Meyer GRA, Roth L, Van der Donckt C, Martinet W, De Meyer GRY, Animal models of atherosclerosis, European Journal of Pharmacology 816 (2017) 3–13. [PubMed: 28483459]

[26]. Hasenfuss G, Animal models of human cardiovascular disease, heart failure and hypertrophy, Cardiovascular Research 39(1) (1998) 60–76. [PubMed: 9764190]

[27]. Russell JC, Proctor SD, Small animal models of cardiovascular disease: tools for the study of the roles of metabolic syndrome, dyslipidemia, and atherosclerosis, Cardiovascular Pathology 15(6) (2006) 318–330. [PubMed: 17113010]

[28]. Hansen BC, Bodkin NL, Primary Prevention of Diabetes Mellitus by Prevention of Obesity in Monkeys, Diabetes 42(12) (1993) 1809–1814. [PubMed: 8243827]

[29]. Hansen BC, The Metabolic Syndrome X, Annals of the New York Academy of Sciences 892(1) (1999) 1–24. [PubMed: 10842649]

[30]. Meyvantsson I, Beebe DJ, Cell Culture Models in Microfluidic Systems, Annual Review of Analytical Chemistry 1(1) (2008) 423–449.

[31]. Farcas MA, Rouleau L, Fraser R, Leask RL, The development of 3-D, in vitro, endothelial culture models for the study of coronary artery disease, BioMedical Engineering OnLine 8(1) (2009) 30. [PubMed: 19863806]

[32]. Rouleau L, Copland IB, Tardif J-C, Mongrain R, Leask RL, Neutrophil Adhesion on Endothelial Cells in a Novel Asymmetric Stenosis Model: Effect of Wall Shear Stress Gradients, Annals of Biomedical Engineering 38(9) (2010) 2791–2804. [PubMed: 20387119]

[33]. Rouleau L, Rossi J, Leask RL, The Response of Human Aortic Endothelial Cells in a Stenotic Hemodynamic Environment: Effect of Duration, Magnitude, and Spatial Gradients in Wall Shear

Stress, Journal of Biomechanical Engineering 132(7) (2010) 071015–071015–11. [PubMed: 20590293]

[34]. Rouleau L, Farcas M, Tardif J-C, Mongrain R, Leask RL, Endothelial Cell Morphologic Response to Asymmetric Stenosis Hemodynamics: Effects of Spatial Wall Shear Stress Gradients, Journal of Biomechanical Engineering 132(8) (2010) 081013–081013–10. [PubMed: 20670062]

[35]. Young EWK, Watson MWL, Srigunapalan S, Wheeler AR, Simmons CA, Technique for Real-Time Measurements of Endothelial Permeability in a Microfluidic Membrane Chip Using Laser-Induced Fluorescence Detection, Analytical Chemistry 82(3) (2010) 808–816. [PubMed: 20050596]

[36]. Kolhar P, Anselmo AC, Gupta V, Pant K, Prabhakarpandian B, Ruoslahti E, Mitragotri S, Using shape effects to target antibody-coated nanoparticles to lung and brain endothelium, Proceedings of the National Academy of Sciences 110(26) (2013) 10753–10758.

[37]. Korin N, Kanapathipillai M, Matthews BD, Crescente M, Brill A, Mammoto T, Ghosh K, Jurek S, Bencherif SA, Bhatta D, Coskun AU, Feldman CL, Wagner DD, Ingber DE, Shear-Activated Nanotherapeutics for Drug Targeting to Obstructed Blood Vessels, Science 337(6095) (2012) 738–742. [PubMed: 22767894]

[38]. Lamberti G, Tang Y, Prabhakarpandian B, Wang Y, Pant K, Kiani MF, Wang B, Adhesive interaction of functionalized particles and endothelium in idealized microvascular networks, Microvascular Research 89 (2013) 107–114. [PubMed: 23557880]

[39]. Doshi N, Prabhakarpandian B, Rea-Ramsey A, Pant K, Sundaram S, Mitragotri S, Flow and adhesion of drug carriers in blood vessels depend on their shape: A study using model synthetic microvascular networks, Journal of Controlled Release 146(2) (2010) 196–200. [PubMed: 20385181]

[40]. Cines DB, Pollak ES, Buck CA, Loscalzo J, Zimmerman GA, McEver RP, Pober JS, Wick TM, Konkle BA, Schwartz BS, Barnathan ES, McCrae KR, Hug BA, Schmidt A-M, Stern DM, Endothelial Cells in Physiology and in the Pathophysiology of Vascular Disorders, Blood 91(10) (1998) 3527–3561. [PubMed: 9572988]

[41]. Jeong Ai K, Nam DT, Zhen L, Fan Y, Weilin Z, Mark JF, Brain Endothelial Hemostasis Regulation by Pericytes, Journal of Cerebral Blood Flow & Metabolism 26(2) (2005) 209–217.

[42]. Grant DS, Tashiro K-I, Segui-Real B, Yamada Y, Martin GR, Kleinman HK, Two different laminin domains mediate the differentiation of human endothelial cells into capillarylike structures in vitro, Cell 58(5) (1989) 933–943. [PubMed: 2528412]

[43]. Morin O, Patry P, Lafleur L, Heterogeneity of endothelial cells of adult rat liver as resolved by sedimentation velocity and flow cytometry, Journal of Cellular Physiology 119(3) (1984) 327–334. [PubMed: 6725418]

[44]. Sankar S, Mahooti-Brooks N, Bensen L, McCarthy TL, Centrella M, Madri JA, Modulation of transforming growth factor beta receptor levels on microvascular endothelial cells during in vitro angiogenesis, Journal of Clinical Investigation 97(6) (1996) 1436–1446. [PubMed: 8617876]

[45]. Cockerill GW, Rye K-A, Gamble JR, Vadas MA, Barter PJ, High-Density Lipoproteins Inhibit Cytokine-Induced Expression of Endothelial Cell Adhesion Molecules, Arteriosclerosis, Thrombosis, and Vascular Biology 15(11) (1995) 1987–1994.

[46]. Owman C, Hardebo JE, Functional Heterogeneity of the Cerebrovascular Endothelium, Brain, Behavior and Evolution 32(2) (1988) 65–75.

[47]. Thornhill MH, Haskard DO, IL-4 regulates endothelial cell activation by IL-1, tumor necrosis factor, or IFN-gamma, The Journal of Immunology 145(3) (1990) 865–872. [PubMed: 1695647]

[48]. Fillinger MF, Sampson LN, Cronenwett JL, Powell RJ, Wagner RJ, Coculture of Endothelial Cells and Smooth Muscle Cells in Bilayer and Conditioned Media Models, Journal of Surgical Research 67(2) (1997) 169–178. [PubMed: 9073564]

[49]. Owens GK, Kumar MS, Wamhoff BR, Molecular regulation of vascular smooth muscle cell differentiation in development and disease, Physiol Rev 84 (2004).

[50]. Beamish JA, He P, Kottke-Marchant K, Marchant RE, Molecular Regulation of Contractile Smooth Muscle Cell Phenotype: Implications for Vascular Tissue Engineering, Tissue Engineering Part B: Reviews 16(5) (2010) 467–491. [PubMed: 20334504]

[51]. Steucke KE, Tracy PV, Hald ES, Hall JL, Alford PW, Vascular smooth muscle cell functional contractility depends on extracellular mechanical properties, Journal of Biomechanics 48(12) (2015) 3044–3051. [PubMed: 26283412]

[52]. Fernandez CE, Yen RW, Perez SM, Bedell HW, Povsic TJ, Reichert WM, Truskey GA, Human Vascular Microphysiological System for in vitro Drug Screening, Scientific Reports 6 (2016) 21579. [PubMed: 26888719]

[53]. Powell RJ, Cronenwett JL, Fillinger MF, Wagner RJ, Effect of endothelial cells and transforming growth factor-ß1 on cultured vascular smooth muscle cell growth patterns, Journal of Vascular Surgery 20(5) (1994) 787–794. [PubMed: 7966814]

[54]. Nackman GB, Bech FR, Fillinger MF, Wagner RJ, Cronenwett JL, Endothelial cells modulate smooth muscle cell morphology by inhibition of transforming growth factor-beta1 activation, Surgery 120(2) (1996) 418–426. [PubMed: 8751613]

[55]. Merrilees MJ, Scott L, Interaction of aortic endothelial and smooth muscle cells in culture Effect on glycosaminoglycan levels, Atherosclerosis 39(2) (1981) 147–161. [PubMed: 7247996]

[56]. Skardal A, Shupe T, Atala A, Organoid-on-a-chip and body-on-a-chip systems for drug screening and disease modeling, Drug Discovery Today 21(9) (2016) 1399–1411. [PubMed: 27422270]

[57]. Bacabac RG, Smit TH, Cowin SC, Van Loon JJWA, Nieuwstadt FTM, Heethaar R, Klein-Nulend J, Dynamic shear stress in parallel-plate flow chambers, Journal of Biomechanics 38(1) 159–167. [PubMed: 15519352]

[58]. Bancroft GN, Sikavitsas VI, Mikos AG, Technical Note: Design of a Flow Perfusion Bioreactor System for Bone Tissue-Engineering Applications, Tissue Engineering 9(3) (2003) 549–554. [PubMed: 12857422]

[59]. Higgins JM, Eddington DT, Bhatia SN, Mahadevan L, Sickle cell vasoocclusion and rescue in a microfluidic device, Proceedings of the National Academy of Sciences 104(51) (2007) 20496–20500.

[60]. Barabino G, McIntire L, Eskin S, Sears D, Udden M, Endothelial cell interactions with sickle cell, sickle trait, mechanically injured, and normal erythrocytes under controlled flow, Blood 70(1) (1987) 152–157. [PubMed: 3593962]

[61]. Nash G, Johnson C, Meiselman H, Rheologic impairment of sickle RBCs induced by repetitive cycles of deoxygenation-reoxygenation, Blood 72(2) (1988) 539–545. [PubMed: 3401593]

[62]. Young EWK, Simmons CA, Macro- and microscale fluid flow systems for endothelial cell biology, Lab on a Chip 10(2) (2010) 143–160. [PubMed: 20066241]

[63]. Young EWK, Beebe DJ, Fundamentals of microfluidic cell culture in controlled microenvironments, Chemical Society Reviews 39(3) (2010) 1036–1048. [PubMed: 20179823]

[64]. Griffith LG, Swartz MA, Capturing complex 3D tissue physiology in vitro, Nature Reviews Molecular Cell Biology 7 (2006) 211. [PubMed: 16496023]

[65]. Schaff UY, Xing MMQ, Lin KK, Pan N, Jeon NL, Simon SI, Vascular mimetics based on microfluidics for imaging the leukocyte-endothelial inflammatory response, Lab on a Chip 7(4) (2007) 448–456. [PubMed: 17389960]

[66]. Ingber DE, Tensegrity I Cell structure and hierarchical systems biology, Journal of Cell Science 116(7) (2003) 1157–1173. [PubMed: 12615960]

[67]. Ingber DE, Tensegrity II. How structural networks influence cellular information processing networks, Journal of Cell Science 116(8) (2003) 1397–1408. [PubMed: 12640025]

[68]. Yasotharan S, Pinto S, Sled JG, Bolz S-S, Gunther A, Artery-on-a-chip platform for automated, multimodal assessment of cerebral blood vessel structure and function, Lab on a Chip 15(12) (2015) 2660–2669. [PubMed: 25990299]

[69]. Ribas J, Sadeghi H, Manbachi A, Leijten J, Brinegar K, Zhang YS, Ferreira L, Khademhosseini A, Cardiovascular Organ-on-a-Chip Platforms for Drug Discovery and Development, Applied In Vitro Toxicology 2(2) (2016) 82–96. [PubMed: 28971113]

[70]. Jain A, van der Meer AD, Papa A-L, Barrile R, Lai A, Schlechter BL, Otieno MA, Louden CS, Hamilton GA, Michelson AD, Frelinger AL, Ingber DE, Assessment of whole blood thrombosis in a microfluidic device lined by fixed human endothelium, Biomedical Microdevices 18 (2016) 73. [PubMed: 27464497]

[71]. Jain A, Munn LL, Biomimetic postcapillary expansions for enhancing rare blood cell separation on a microfluidic chip, Lab on a Chip 11(17) (2011) 2941–2947. [PubMed: 21773633]

[72]. Jain A, Graveline A, Waterhouse A, Vernet A, Flaumenhaft R, Ingber DE, A shear gradient-activated microfluidic device for automated monitoring of whole blood haemostasis and platelet function, Nature Communications 7 (2016) 10176.

[73]. Benam KH, Dauth S, Hassell B, Herland A, Jain A, Jang K-J, Karalis K, Kim HJ, MacQueen L, Mahmoodian R, Musah S, Torisawa Y.-s., Meer A.D.v.d., Villenave R, Yadid M, Parker KK, Ingber DE, Engineered In Vitro Disease Models, Annual Review of Pathology: Mechanisms of Disease 10(1) (2015) 195–262.

[74]. Westein E, van der Meer AD, Kuijpers MJE, Frimat J-P, van den Berg A, Heemskerk JWM, Atherosclerotic geometries exacerbate pathological thrombus formation poststenosis in a von Willebrand factor-dependent manner, Proceedings of the National Academy of Sciences 110(4) (2013) 1357–1362.

[75]. Zhang YS, Davoudi F, Walch P, Manbachi A, Luo X, Dell'Erba V, Miri AK, Albadawi H, Arneri A, Li X, Wang X, Dokmeci MR, Khademhosseini A, Oklu R, Bioprinted thrombosis-on-a-chip, Lab on a Chip 16(21) (2016) 4097–4105. [PubMed: 27722710]

[76]. Bertassoni LE, Cecconi M, Manoharan V, Nikkhah M, Hjortnaes J, Cristino AL, Barabaschi G, Demarchi D, Dokmeci MR, Yang Y, Khademhosseini A, Hydrogel bioprinted microchannel networks for vascularization of tissue engineering constructs, Lab on a Chip 14(13) (2014) 2202–2211. [PubMed: 24860845]

[77]. Barrile R, van der Meer AD, Park H, Fraser JP, Simic D, Teng F, Conegliano D, Nguyen J, Jain A, Zhou M, Organ-on-Chip Recapitulates Thrombosis Induced by an anti-CD154 Monoclonal Antibody: Translational Potential of Advanced Microengineered Systems, Clinical Pharmacology & Therapeutics (2018).

[78]. Alimperti S, Mirabella T, Bajaj V, Polacheck W, Pirone DM, Duffield J, Eyckmans J, Assoian RK, Chen CS, Three-dimensional biomimetic vascular model reveals a RhoA, Rac1, and N-cadherin balance in mural cell–endothelial cell-regulated barrier function, Proceedings of the National Academy of Sciences (2017).

[79]. Thomas A, Daniel Ou-Yang H, Lowe-Krentz L, Muzykantov VR, Liu Y, Biomimetic channel modeling local vascular dynamics of pro-inflammatory endothelial changes, Biomicrofluidics 10(1) (2016) 014101. [PubMed: 26858813]

[80]. Park JY, Kim HO, Kim K-D, Kim SK, Lee SK, Jung H, Monitoring the status of Tcell activation in a microfluidic system, Analyst 136(13) (2011) 2831–2836. [PubMed: 21623432]

[81]. Kim S, Lee H, Chung M, Jeon NL, Engineering of functional, perfusable 3D microvascular networks on a chip, Lab on a Chip 13(8) (2013) 1489–1500. [PubMed: 23440068]

[82]. Fredrickson CK, Fan ZH, Macro-to-micro interfaces for microfluidic devices, Lab on a Chip 4(6) (2004) 526–533. [PubMed: 15570361]

[83]. Whitesides GM, The origins and the future of microfluidics, Nature 442 (2006) 368. [PubMed: 16871203]

[84]. Muthard RW, Diamond SL, Side view thrombosis microfluidic device with controllable wall shear rate and transthrombus pressure gradient, Lab on a Chip 13(10) (2013) 1883–1891. [PubMed: 23549358]

[85]. Chueh B.-h., Huh D, Kyrtsos CR, Houssin T, Futai N, Takayama S, Leakage-Free Bonding of Porous Membranes into Layered Microfluidic Array Systems, Analytical Chemistry 79(9) (2007) 3504–3508. [PubMed: 17388566]

[86]. Shery Huang YY, Zhang D, Liu Y, Bioprinting of three-dimensional culture models and organ-on-a-chip systems, MRS Bulletin 42(8) (2017) 593–599.

[87]. Wang X, Phan DTT, Sobrino A, George SC, Hughes CCW, Lee AP, Engineering anastomosis between living capillary networks and endothelial cell-lined microfluidic channels, Lab on a Chip 16(2) (2016) 282–290. [PubMed: 26616908]

[88]. Memic A, Navaei A, Mirani B, Cordova JAV, Aldhahri M, Dolatshahi-Pirouz A, Akbari M, Nikkhah M, Bioprinting technologies for disease modeling, Biotechnology Letters 39(9) (2017) 1279–1290. [PubMed: 28550360]

[89]. A.S. F2792–12A, Standard Terminology for additive manufacturing technologies, ASTM International (2013).

[90]. Zhao X, Irvine SA, Agrawal A, Cao Y, Lim PQ, Tan SY, Venkatraman SS, 3D patterned substrates for bioartificial blood vessels – The effect of hydrogels on aligned cells on a biomaterial surface, Acta Biomaterialia 26 (2015) 159–168. [PubMed: 26297885]

[91]. Irvine S, Venkatraman S, Bioprinting and Differentiation of Stem Cells, Molecules 21(9) (2016) 1188.

[92]. Bobak M, Guanglei X, Simon D, James KM, Current progress in 3D printing for cardiovascular tissue engineering, Biomedical Materials 10(3) (2015) 034002. [PubMed: 25775166]

[93]. Vukicevic M, Mosadegh B, Min JK, Little SH, Cardiac 3D Printing and its Future Directions, JACC: Cardiovascular Imaging 10(2) (2017) 171–184. [PubMed: 28183437]

[94]. Swati G, Alpa B, Manish C, Shivaji M, Bhadra T, Vishal PC, Narayan S, Sarang G, Vijay A, Clinical Application and Multidisciplinary Assessment of Three Dimensional Printing in Double Outlet Right Ventricle With Remote Ventricular Septal Defect, World Journal for Pediatric and Congenital Heart Surgery 7(3) (2016) 344–350. [PubMed: 27142402]

[95]. Niklason LE, Gao J, Abbott WM, Hirschi KK, Houser S, Marini R, Langer R, Functional Arteries Grown in Vitro, Science 284(5413) (1999) 489–493. [PubMed: 10205057]

[96]. Laflamme K, Roberge CJ, Labonté J, Pouliot S, D'Orléans-Juste P, Auger FA, Germain L, Tissue-Engineered Human Vascular Media With a Functional Endothelin System, Circulation 111(4) (2005) 459–464. [PubMed: 15687134]

[97]. Laflamme K, Roberge CJ, Grenier G, Rémy-Zolghadri M, Pouliot S, Baker K, Labbé R, D'Orléans-Juste P, Auger FA, Germain L, Adventitia contribution in vascular tone: insights from adventitia-derived cells in a tissue-engineered human blood vessel, The FASEB Journal 20(8) (2006) 1245–1247. [PubMed: 16611833]

[98]. Diebolt M, Laflamme K, Labbé R, Auger FA, Germain L, Andriantsitohaina R, Polyphenols modulate calcium-independent mechanisms in human arterial tissue-engineered vascular media, Journal of Vascular Surgery 46(4) (2007) 764–772. [PubMed: 17764876]

[99]. Diebolt M, Germain L, Auger FA, Andriantsitohaina R, Mechanism of potentiation by polyphenols of contraction in human vein-engineered media, American Journal of PhysiologyHeart and Circulatory Physiology 288(6) (2005) H2918–H2924.

[100]. Pricci M, Bourget J-M, Robitaille H, Porro C, Soleti R, Mostefai HA, Auger FA, Martinez MC, Andriantsitohaina R, Germain L, Applications of Human Tissue-Engineered Blood Vessel Models to Study the Effects of Shed Membrane Microparticles from TLymphocytes on Vascular Function, Tissue Engineering Part A 15(1) (2009) 137–145. [PubMed: 18925833]

[101]. K. MA, Daniel N, Luis I, Hossein GH, Sushila M, U. REG, Parastoo K, Amir M, Remzi DM, Shaochen C, Ryon SS, Shrike ZY, Ali K, Microfluidics-Enabled Multimaterial Maskless Stereolithographic Bioprinting, Advanced Materials 0(0) 1800242.

[102]. Massa S, Sakr M, Seo J, Bandaru P, Arneri A, Bersini S, Zare Eelanjegh E, Jalilian E, Cha B-H, Antona S, Enrico A, Gao Y, Hassan S, Acevedo J, Dokmeci M, Zhang Y, Khademhosseini A, Shin S, Bioprinted 3D vascularized tissue model for drug toxicity analysis, Biomicrofluidics 11(4) (2017) 044109. [PubMed: 28852429]

[103]. Kang H-W, Lee SJ, Ko IK, Kengla C, Yoo JJ, Atala A, A 3D bioprinting system to produce human-scale tissue constructs with structural integrity, Nat Biotech 34(3) (2016) 312–319.

[104]. Xiong G, Kolli K, Soohoo HA, Min JK, Abstract 19898: In-vitro Assessment of Coronary Hemodynamics in 3D Printed Patient-specific Geometry, Circulation 132(Suppl 3) (2015) A19898–A19898.

[105]. Kolli KK, Min JK, Ha S, Soohoo H, Xiong G, Effect of Varying Hemodynamic and Vascular Conditions on Fractional Flow Reserve: An In Vitro Study, Journal of the American Heart Association 5(7) (2016).

[106]. Kolesky DB, Homan KA, Skylar-Scott MA, Lewis JA, Three-dimensional bioprinting of thick vascularized tissues, Proceedings of the National Academy of Sciences 113(12) (2016) 3179–3184.

[107]. Ouyang L, Highley CB, Rodell CB, Sun W, Burdick JA, 3D Printing of ShearThinning Hyaluronic Acid Hydrogels with Secondary Cross-Linking, ACS Biomaterials Science & Engineering 2(10) (2016) 1743–1751.

[108]. Itoh M, Nakayama K, Noguchi R, Kamohara K, Furukawa K, Uchihashi K, Toda S, Oyama J.i., Node K, Morita S, Scaffold-Free Tubular Tissues Created by a Bio-3D Printer Undergo Remodeling and Endothelialization when Implanted in Rat Aortae, PLOS ONE 10(9) (2015) e0136681. [PubMed: 26325298]

[109]. Iwasaki K, Kojima K, Kodama S, Paz AC, Chambers M, Umezu M, Vacanti CA, Bioengineered Three-Layered Robust and Elastic Artery Using Hemodynamically-Equivalent Pulsatile Bioreactor, Circulation 118(14 suppl 1) (2008) S52–S57. [PubMed: 18824769]

[110]. Tsai KJ, Dixon S, Hale LR, Darbyshire A, Martin D, de Mel A, Biomimetic heterogenous elastic tissue development, npj Regenerative Medicine 2(1) (2017) 16.

[111]. Carrow JK, Kerativitayanan P, Jaiswal MK, Lokhande G, Gaharwar AK, Chapter 13 - Polymers for Bioprinting A2 - Atala, Anthony, in: Yoo JJ (Ed.), Essentials of 3D Biofabrication and Translation, Academic Press, Boston, 2015, pp. 229–248.

[112]. Gao Q, Liu Z, Lin Z, Qiu J, Liu Y, Liu A, Wang Y, Xiang M, Chen B, Fu J, He Y, 3D Bioprinting of Vessel-like Structures with Multilevel Fluidic Channels, ACS Biomaterials Science & Engineering 3(3) (2017) 399–408.

[113]. Peak CW, Stein J, Gold KA, Gaharwar AK, Nanoengineered Colloidal Inks for 3D Bioprinting, Langmuir (2017).

[114]. Chimene D, Peak CW, Gentry JL, Carrow JK, Cross LM, Mondragon E, Cardoso GB, Kaunas R, Gaharwar AK, Nanoengineered Ionic–Covalent Entanglement (NICE) Bioinks for 3D Bioprinting, ACS Applied Materials & Interfaces 10(12) (2018) 9957–9968. [PubMed: 29461795]

[115]. Hockaday LA, Kang KH, Colangelo NW, Cheung PYC, Duan B, Malone E, Wu J, Girardi LN, Bonassar LJ, Lipson H, Chu CC, Butcher JT, Rapid 3D printing of anatomically accurate and mechanically heterogeneous aortic valve hydrogel scaffolds, Biofabrication 4(3) (2012) 035005. [PubMed: 22914604]

[116]. Xiaoxiao H, Richard B, Russell H, Engineering design of artificial vascular junctions for 3D printing, Biofabrication 8(2) (2016) 025018. [PubMed: 27321286]

[117]. Shin SR, Jung SM, Zalabany M, Kim K, Zorlutuna P, Kim S.b., Nikkhah M, Khabiry M, Azize M, Kong J, Wan K.-t., Palacios T, Dokmeci MR, Bae H, Tang X, Khademhosseini A, Carbon-Nanotube-Embedded Hydrogel Sheets for Engineering Cardiac Constructs and Bioactuators, ACS Nano 7(3) (2013) 2369–2380. [PubMed: 23363247]

[118]. Izadifar M, Chapman D, Babyn P, Chen X, Kelly ME, UV-Assisted 3D Bioprinting of Nanoreinforced Hybrid Cardiac Patch for Myocardial Tissue Engineering, Tissue Engineering Part C: Methods 24(2) (2017) 74–88. [PubMed: 29050528]

[119]. Paul A, Hasan A, Kindi HA, Gaharwar AK, Rao VTS, Nikkhah M, Shin SR, Krafft D, Dokmeci MR, Shum-Tim D, Khademhosseini A, Injectable Graphene Oxide/Hydrogel-Based Angiogenic Gene Delivery System for Vasculogenesis and Cardiac Repair, ACS Nano 8(8) (2014) 8050–8062. [PubMed: 24988275]

[120]. Navaei A, Saini H, Christenson W, Sullivan RT, Ros R, Nikkhah M, Gold nanorodincorporated gelatin-based conductive hydrogels for engineering cardiac tissue constructs, Acta Biomaterialia 41 (2016) 133–146. [PubMed: 27212425]

[121]. Wilson SA, Cross LM, Peak CW, Gaharwar AK, Shear-Thinning and Thermo-Reversible Nanoengineered Inks for 3D Bioprinting, ACS applied materials & interfaces 9(50) (2017) 43449–43458. [PubMed: 29214803]

[122]. Chimene D, Alge DL, Gaharwar AK, Two-dimensional nanomaterials for biomedical applications: emerging trends and future prospects, Adv Mater 27(45) (2015) 7261–7284. [PubMed: 26459239]

[123]. Cross LM, Shah K, Palani S, Peak CW, Gaharwar AK, Gradient nanocomposite hydrogels for interface tissue engineering, Nanomedicine: Nanotechnology, Biology and Medicine (2017).

[124]. Lokhande G, Carrow JK, Thakur T, Xavier JR, Parani M, Bayless KJ, Gaharwar AK, Nanoengineered injectable hydrogels for wound healing application, Acta biomaterialia (2018).

[125]. Murphy SV, Atala A, 3D bioprinting of tissues and organs, Nature Biotechnology 32 (2014) 773.

[126]. C. SB, G. LJ, M. SA, A. GK, S. WT, J. WS, Elizabeth CH, H. WJ, Hemostatic and Absorbent PolyHIPE–Kaolin Composites for 3D Printable Wound Dressing Materials, Macromolecular Bioscience 18(5) (2018) 1700414.

[127]. A. SN, S. DP, M. CHE, Emulsion Inks for 3D Printing of High Porosity Materials, Macromolecular Rapid Communications 37(16) (2016) 1369–1374. [PubMed: 27305061]

[128]. Ding H, Chang R, Printability Study of Bioprinted Tubular Structures Using Liquid Hydrogel Precursors in a Support Bath, Applied Sciences 8(3) (2018) 403.

[129]. Jin Y, Chai W, Huang Y, Printability study of hydrogel solution extrusion in nanoclay yield-stress bath during printing-then-gelation biofabrication, Materials Science and Engineering: C 80 (2017) 313–325. [PubMed: 28866170]

[130]. Jin Y, Compaan A, Chai W, Huang Y, Functional Nanoclay Suspension for Printing-Then-Solidification of Liquid Materials, ACS Applied Materials & Interfaces 9(23) (2017) 20057–20066. [PubMed: 28534614]

[131]. Rocca M, Fragasso A, Liu W, Heinrich MA, Zhang YS, Embedded Multimaterial Extrusion Bioprinting, SLAS TECHNOLOGY: Translating Life Sciences Innovation 0(0) 2472630317742071.

[132]. Chimene D, Lennox KK, Kaunas RR, Gaharwar AK, Advanced Bioinks for 3D Printing: A Materials Science Perspective, Annals of Biomedical Engineering 44(6) (2016) 2090–2102. [PubMed: 27184494]

[133]. Jang J, Park H-J, Kim S-W, Kim H, Park JY, Na SJ, Kim HJ, Park MN, Choi SH, Park SH, Kim SW, Kwon S-M, Kim P-J, Cho D-W, 3D printed complex tissue construct using stem cell-laden decellularized extracellular matrix bioinks for cardiac repair, Biomaterials 112 (2017) 264–274. [PubMed: 27770630]

[134]. Weining B, Christopher PJ, Nenad B, Controlling the structural and functional anisotropy of engineered cardiac tissues, Biofabrication 6(2) (2014) 024109. [PubMed: 24717534]

[135]. Wang MO, Vorwald CE, Dreher ML, Mott EJ, Cheng M-H, Cinar A, Mehdizadeh H, Somo S, Dean D, Brey EM, Fisher JP, Evaluating 3D Printed Biomaterials as Scaffolds for Vascularized Bone Tissue Engineering, Advanced materials (Deerfield Beach, Fla.) 27(1) (2015) 138–144.

[136]. Ajay T, Scott Alexander I, Udi S, Priyadarshini M, Vrushali B, Subbu V, Contact guidance for cardiac tissue engineering using 3D bioprinted gelatin patterned hydrogel, Biofabrication 10(2) (2018) 025003. [PubMed: 29235444]

[137]. Wang Z, Lee SJ, Cheng H-J, Yoo JJ, Atala A, 3D bioprinted functional and contractile cardiac tissue constructs, Acta Biomaterialia (2018).

[138]. Cooper SL, Peppas NA, Hoffman AS, Ratner BD, Biomaterials: Interfacial Phenomena and Applications, AMERICAN CHEMICAL SOCIETY1982.

[139]. Daniel R, Wenkai J, Dhavan S, Kemin F, Guifang W, Jeremy G, Feng Z, Tissue Engineering at the Blood-Contacting Surface: A Review of Challenges and Strategies in Vascular Graft Development, Advanced Healthcare Materials 0(0) 1701461.

[140]. Sandip S, M. SK, George H, M. SA, Addressing thrombogenicity in vascular graft construction, Journal of Biomedical Materials Research Part B: Applied Biomaterials 82B(1) (2007) 100–108.

[141]. Hulander M, Lundgren A, Faxälv L, Lindahl TL, Palmquist A, Berglin M, Elwing H, Gradients in surface nanotopography used to study platelet adhesion and activation, Colloids and Surfaces B: Biointerfaces 110 (2013) 261–269. [PubMed: 23732803]

[142]. F. HJ, O. ER, Effects of roughness on the thrombogenicity of a plastic, Journal of Biomedical Materials Research 15(1) (1981) 1–7. [PubMed: 7348699]

[143]. Milleret V, Hefti T, Hall H, Vogel V, Eberli D, Influence of the fiber diameter and surface roughness of electrospun vascular grafts on blood activation, Acta Biomaterialia 8(12) (2012) 4349–4356. [PubMed: 22842036]

[144]. Kee MF, Myers DR, Sakurai Y, Lam WA, Qiu Y, Platelet Mechanosensing of Collagen Matrices, PLOS ONE 10(4) (2015) e0126624. [PubMed: 25915413]

[145]. Qiu Y, Brown AC, Myers DR, Sakurai Y, Mannino RG, Tran R, Ahn B, Hardy ET, Kee MF, Kumar S, Bao G, Barker TH, Lam WA, Platelet mechanosensing of substrate stiffness during clot

formation mediates adhesion, spreading, and activation, Proceedings of the National Academy of Sciences 111(40) (2014) 14430–14435.

[146]. Qiu Y, Ciciliano J, Myers DR, Tran R, Lam WA, Platelets and physics: How platelets "feel" and respond to their mechanical microenvironment, Blood Reviews 29(6) (2015) 377–386. [PubMed: 26005062]

[147]. Daamen WF, Veerkamp JH, van Hest JCM, van Kuppevelt TH, Elastin as a biomaterial for tissue engineering, Biomaterials 28(30) (2007) 4378–4398. [PubMed: 17631957]

[148]. Kumar VA, Caves JM, Haller CA, Dai E, Liu L, Grainger S, Chaikof EL, Acellular vascular grafts generated from collagen and elastin analogs, Acta Biomaterialia 9(9) (2013) 8067–8074. [PubMed: 23743129]

[149]. Anna G, Han BY, Harvey J, Fazal M, Donald M, Jan F, Wan KS, Heparin release from thermosensitive polymer coatings: in vivo studies, Journal of Biomedical Materials Research 29(7) (1995) 811–821.

[150]. Yali L, G. NK, T. KE, Controlled release of heparin from polypyrrole-poly(vinyl alcohol) assembly by electrical stimulation, Journal of Biomedical Materials Research Part A 73A(2) (2005) 171–181.

[151]. Kharaziha M, Memic A, Akbari M, Brafman DA, Nikkhah M, Nano-Enabled Approaches for Stem Cell-Based Cardiac Tissue Engineering, Advanced Healthcare Materials 5(13) (2016) 1533–1553. [PubMed: 27199266]

[152]. Thavandiran N, Nunes SS, Xiao Y, Radisic M, Topological and electrical control of cardiac differentiation and assembly, Stem Cell Research & Therapy 4(1) (2013) 14. [PubMed: 23425700]

[153]. Fukunishi T, Best CA, Sugiura T, Opfermann J, Ong CS, Shinoka T, Breuer CK, Krieger A, Johnson J, Hibino N, Preclinical study of patient-specific cell-free nanofiber tissueengineered vascular grafts using 3-dimensional printing in a sheep model, The Journal of Thoracic and Cardiovascular Surgery 153(4) (2017) 924–932. [PubMed: 27938900]

[154]. Kolesky DB, Truby RL, Gladman AS, Busbee TA, Homan KA, Lewis JA, 3D Bioprinting of Vascularized, Heterogeneous Cell-Laden Tissue Constructs, Advanced Materials 26(19) (2014) 3124–3130. [PubMed: 24550124]

[155]. Wu W, Hansen CJ, Aragon AM, Geubelle PH, White SR, Lewis JA, Direct-write assembly of biomimetic microvascular networks for efficient fluid transport, Soft Matter 6(4) (2010) 739–742.

[156]. Willie W, Adam D, A. LJ, Omnidirectional Printing of 3D Microvascular Networks, Advanced Materials 23(24) (2011) H178–H183. [PubMed: 21438034]

[157]. Ouyang L, Burdick JA, Sun W, Facile Biofabrication of Heterogeneous Multilayer Tubular Hydrogels by Fast Diffusion-Induced Gelation, ACS Applied Materials & Interfaces 10(15) (2018) 12424–12430. [PubMed: 29582989]

[158]. Carrow JK, Cross LM, Reese RW, Jaiswal MK, Gregory CA, Kaunas R, Singh I, Gaharwar AK, Widespread changes in transcriptome profile of human mesenchymal stem cells induced by two-dimensional nanosilicates, Proceedings of the National Academy of Sciences 115(17) (2018) E3905–E3913.

[159]. Makris EA, Gomoll AH, Malizos KN, Hu JC, Athanasiou KA, Repair and tissue engineering techniques for articular cartilage, Nature Reviews Rheumatology 11 (2014) 21. [PubMed: 25247412]

[160]. Huh D, Kim HJ, Fraser JP, Shea DE, Khan M, Bahinski A, Hamilton GA, Ingber DE, Microfabrication of human organs-on-chips, Nature Protocols 8 (2013) 2135. [PubMed: 24113786]

[161]. Costa PF, Albers HJ, Linssen JEA, Middelkamp HHT, van der Hout L, Passier R, van den Berg A, Malda J, van der Meer AD, Mimicking arterial thrombosis in a 3D-printed microfluidic in vitro vascular model based on computed tomography angiography data, Lab on a Chip 17(16) (2017) 2785–2792. [PubMed: 28717801]

[162]. Hoon SK, B. HC, Andrew R, A. BJ, Complex 3D-Printed Microchannels within Cell-Degradable Hydrogels, Advanced Functional Materials 0(0) 1801331.

[163]. Reardon S, 'Organs-on-chips' go mainstream, Nature 523 (2015).

[164]. Qiu Y, Ahn B, Sakurai Y, Hansen CE, Tran R, Mimche PN, Mannino RG, Ciciliano JC, Lamb TJ, Joiner CH, Ofori-Acquah SF, Lam WA, Microvasculature-on-a-chip for the long-term study of endothelial barrier dysfunction and microvascular obstruction in disease, Nature Biomedical Engineering 2(6) (2018) 453–463.

[165]. Alimperti S, Mirabella T, Bajaj V, Polacheck W, Pirone DM, Duffield J, Eyckmans J, Assoian RK, Chen CS, Three-dimensional biomimetic vascular model reveals a RhoA, Rac1, and N-cadherin balance in mural cell–endothelial cell-regulated barrier function, Proceedings of the National Academy of Sciences 114(33) (2017) 8758–8763.

[166]. Gunther A, Yasotharan S, Vagaon A, Lochovsky C, Pinto S, Yang J, Lau C, Voigtlaender-Bolz J, Bolz S-S, A microfluidic platform for probing small artery structure and function, Lab on a Chip 10(18) (2010) 2341–2349. [PubMed: 20603685]

[167]. Jain A, Barrile R, van der Meer AD, Mammoto A, Mammoto T, De Ceunynck K, Aisiku O, Otieno MA, Louden CS, Hamilton GA, Flaumenhaft R, Ingber DE, A primary human lung alveolus-on-a-chip model of intravascular thrombosis for assessment of therapeutics, Clinical Pharmacology & Therapeutics n/a-n/a.

[168]. Janna CN, Lisa LS, Ryan TH, Jason T, John PF, Jr., Sean PS, Alex C, Suraj K, Ilona S, Josue AG, Patrick HC, Kevin Kit P, Automated fabrication of photopatterned gelatin hydrogels for organ-on-chips applications, Biofabrication 10(2) (2018) 025004.

[169]. van Engeland NCA, Pollet AMAO, den Toonder JMJ, Bouten CVC, Stassen OMJA, Sahlgren CM, A biomimetic microfluidic model to study signalling between endothelial and vascular smooth muscle cells under hemodynamic conditions, Lab on a Chip 18(11) (2018) 1607–1620. [PubMed: 29756630]

[170]. Holzapfel GA, Sommer G, Gasser CT, Regitnig P, Determination of layer-specific mechanical properties of human coronary arteries with nonatherosclerotic intimal thickening and related constitutive modeling, American Journal of Physiology - Heart and Circulatory Physiology 289(5) (2005) H2048–H2058. [PubMed: 16006541]

[171]. Armentano RL, Levenson J, Barra JG, Fischer EI, Breitbart GJ, Pichel RH, Simon A, Assessment of elastin and collagen contribution to aortic elasticity in conscious dogs, American Journal of Physiology-Heart and Circulatory Physiology 260(6) (1991) H1870–H1877.

[172]. Jang S-H, Park Y-L, Yin H, Influence of Coalescence on the Anisotropic Mechanical and Electrical Properties of Nickel Powder/Polydimethylsiloxane Composites, Materials 9(4) (2016) 239.

[173]. Palchesko RN, Zhang L, Sun Y, Feinberg AW, Development of Polydimethylsiloxane Substrates with Tunable Elastic Modulus to Study Cell Mechanobiology in Muscle and Nerve, PLOS ONE 7(12) (2012) e51499. [PubMed: 23240031]

[174]. Carrillo F, Gupta S, Balooch M, Marshall SJ, Marshall GW, Pruitt L, Puttlitz CM, Nanoindentation of polydimethylsiloxane elastomers: Effect of crosslinking, work of adhesion, and fluid environment on elastic modulus, Journal of Materials Research 20(10) (2011) 2820–2830.

[175]. Montini-Ballarin F, Calvo D, Caracciolo PC, Rojo F, Frontini PM, Abraham GA, Guinea GV, Mechanical behavior of bilayered small-diameter nanofibrous structures as biomimetic vascular grafts, Journal of the Mechanical Behavior of Biomedical Materials 60 (2016) 220–233. [PubMed: 26872337]
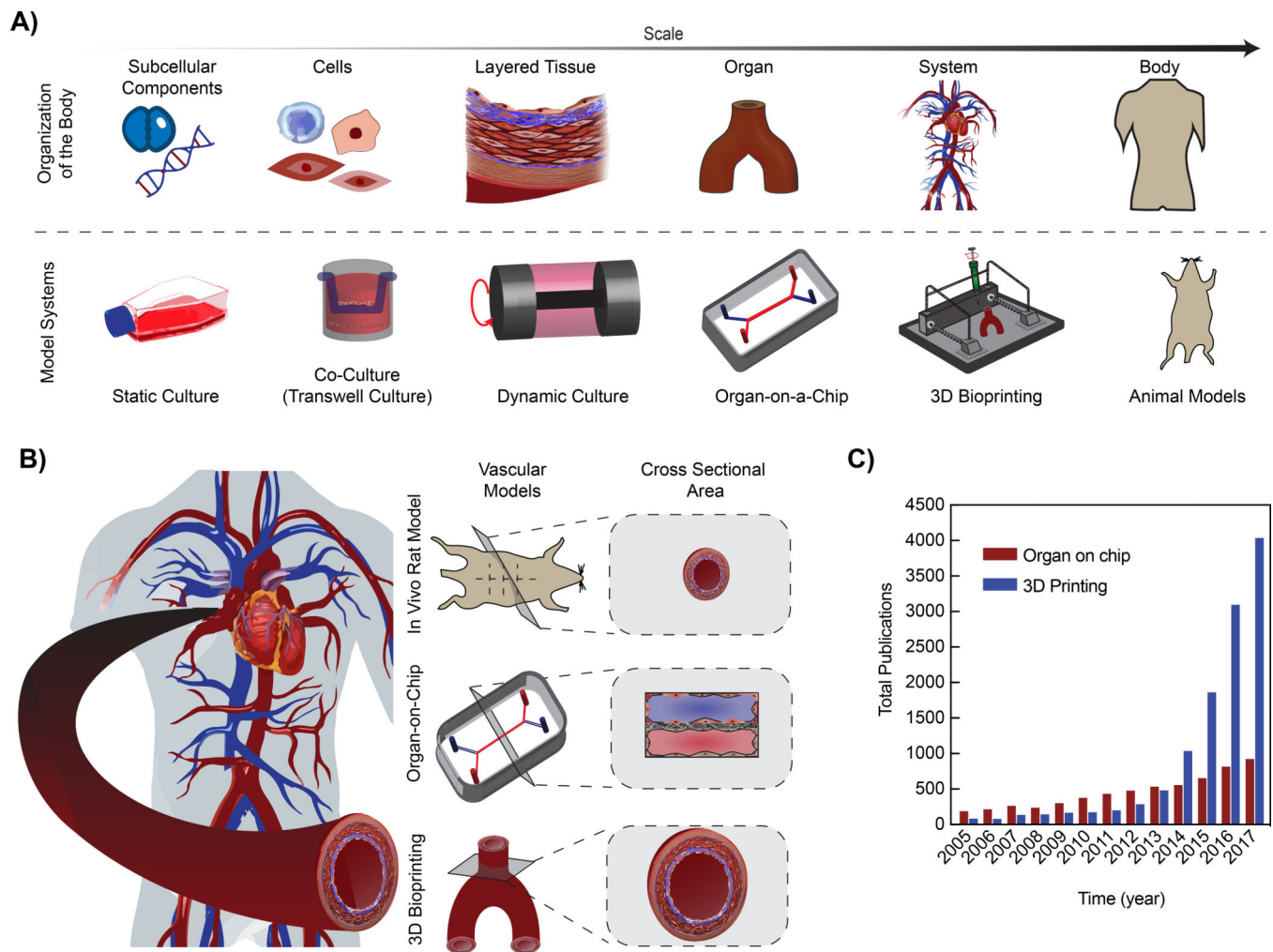
Author Manuscript Author Manuscript Author Manuscript Author Manuscript

Figure 1: Existing and emerging multiscale models of vascular diseases.
A) Schematic illustrating the model systems used to replicate the organization of the body. As the scale increases from subcellular components to the body, the modeling modalities increase in complexity and decrease in the biochemical tools available to assess the model. **B**) The human vasculature system can be modeled using the standard *in vivo* rodent model (smaller crosssectional area), organ-on-chip technology (rectangular cross-sectional area), and 3D Bioprinting (mimics the innate human vascular system). **C**) Number of publications related to "vascular models" over the past 12-years, with search keywords "3D Printing or Additive Manufacturing or 3D Bioprinting and Vascular Model" and "Organ-on-chip or Microphysiological System or Tissue chip and Vascular Model" according to ISI Web of Science (Data obtained in July 2018).
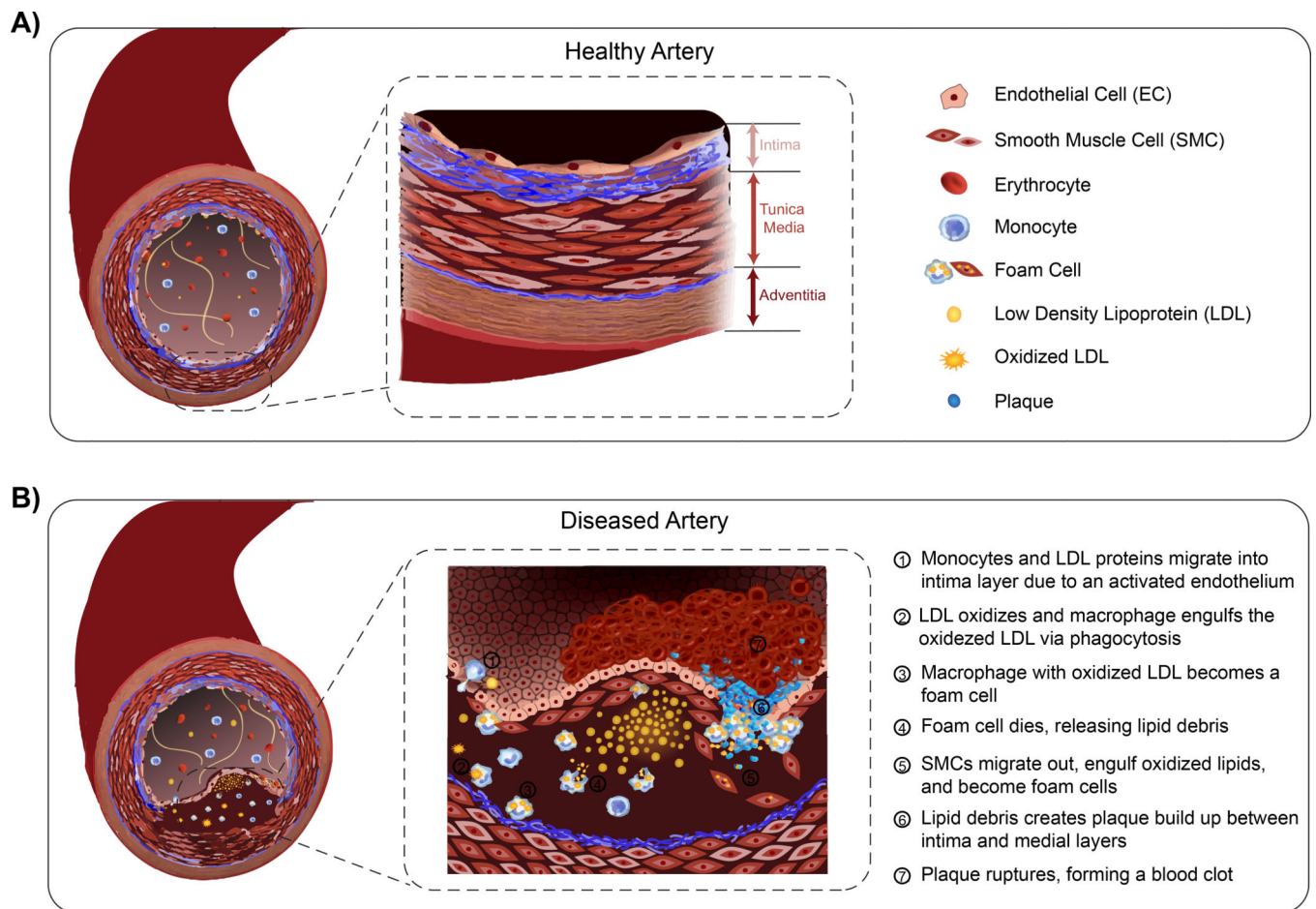
Figure 2: Complex composition of an artery

A) Basic anatomy of a healthy, human arterial blood vessel, containing the intima, tunica media, and adventitia layer. **B**) Illustration of the complex pathophysiological development and progression of vascular disease causing a structural and functional change in arteries.
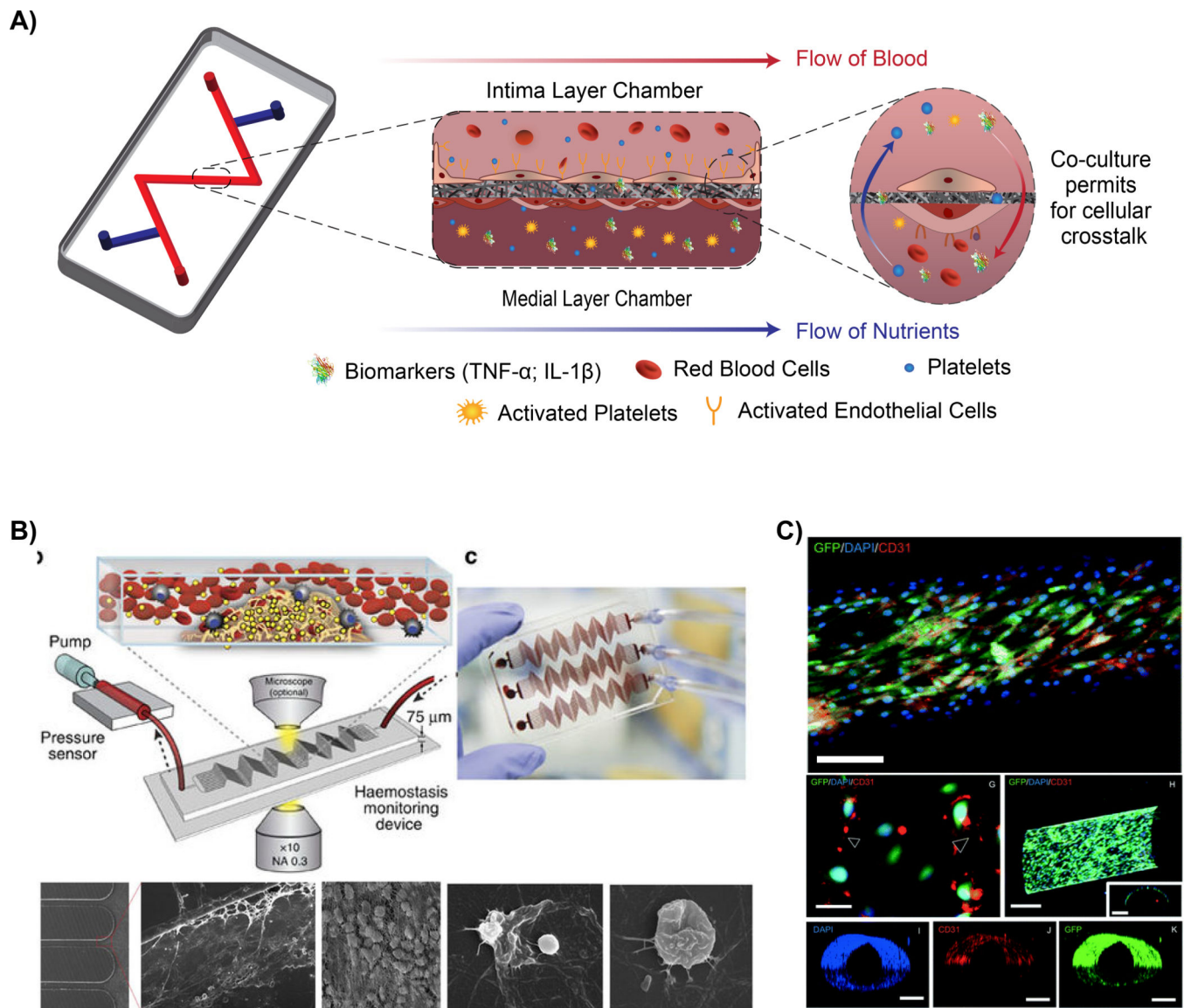
Figure 3: Vascular organ-on-a-chip models.

A) Illustration depicting the cellular communication and dynamic environment within a multi-chamber organ-on-a-chip. **B**) Schematic depicting a hemostasis organ-on-a-chip device, top left. Exposure of blood flow within the microfluidic channel permits for determination of clotting time and the high throughput potential of organ-on-a-chip devices. Scanning electron micrographs of blood clot formation within the device, bottom, illustrating fibrin networks with red blood cell (3 left images) and activated platelets (2 images at right).[72] © 2016 Nature Communications **C**) Confocal image of GFP/DAPI/CD31 biomarkers from endothelial cell monolayer inside microchannel, depicting cellular interactions. (Top – Scale bar 250 μm; G – Scale bar 50 μm; H, I, J, and K – Scale bar 250 μm) [76] © 2014 Lab on Chip
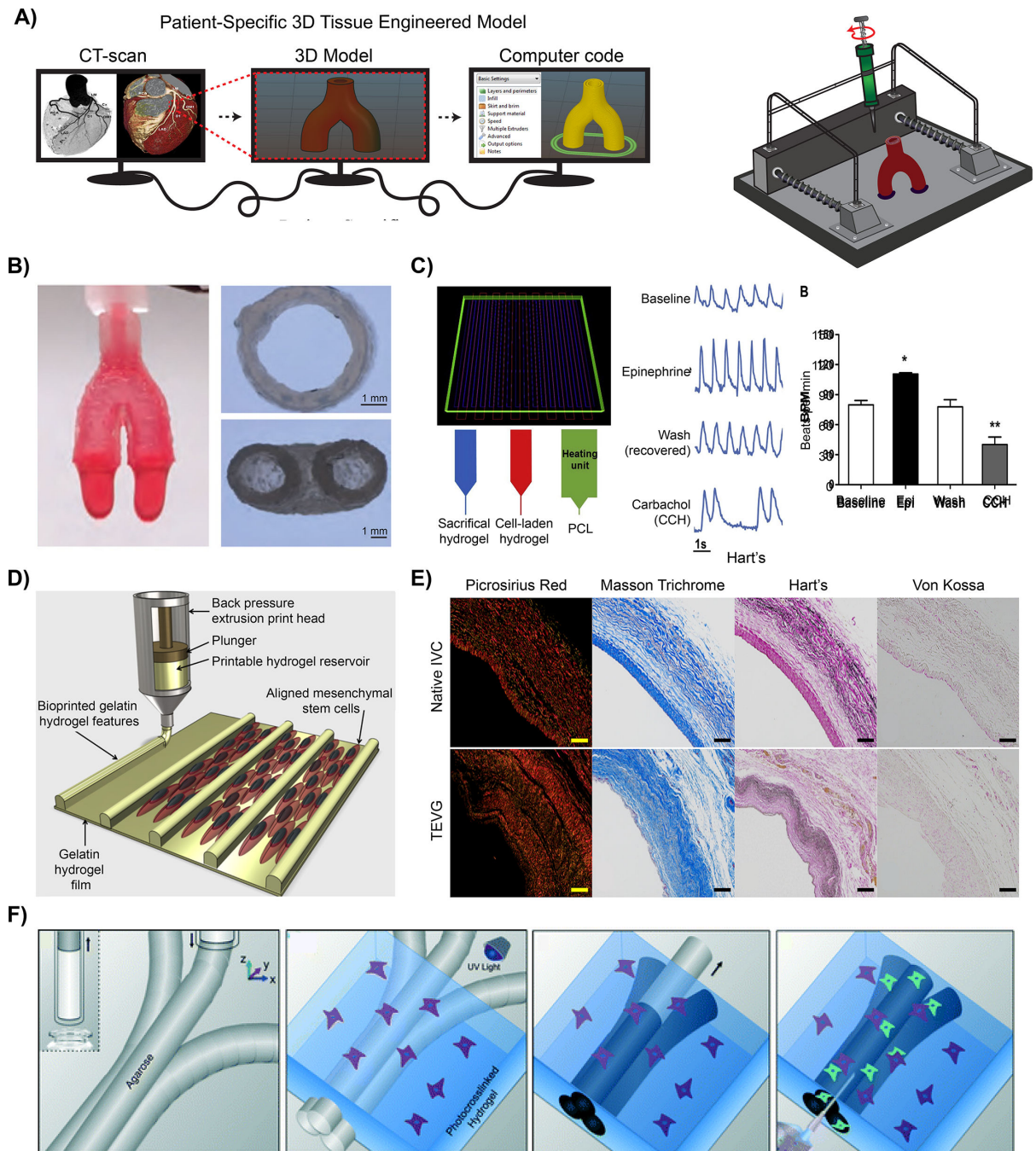
Figure 4: Vascular 3D printed models.
A) Schematic demonstrating the process of fabricating a patient-specific complex geometry using the layer-by-layer 3D printing process. **B)** A bioink utilizing Nanoengineered Ionic-Covalent Entanglements (NICE) improves the hydrogels printability, producing stiff and elastomeric constructs that are physiologically relevant at modeling macroscale organ biology.[114] © 2018 ACS Applied Materials & Interfaces **C)** 3D printing of 3-component cardiac tissue to demonstrate the feasibility of cardiac model drug response. The printed cardiac tissue increased in beating frequency (beats per minute; BPM) and amplitude,

compared to the baseline, when exposed to epinephrine (Epi). However, once removed, washed, established baseline, and then exposed to Carbachol (CCH), the opposite effect was confirmed. [137] © 2018 Acta Biomaterialia **D)** Schematic of the manufacturing process used to produce hydrogel printed microchannels that aid in cellular alignment, mimicking the arrangement observed *in vivo*.[136] © 2018 Biofabrication **E)** Collagen (Picrosirius Red and Masson Trichrome) and elastin (Hart) deposition of a native inferior vena cava (IVC) compared to a 3D printed tissue engineered vascular graft (TEVG) after 6 months. No signs of ectopic calcification were demonstrated (Von Kossa).[153] © 2017 The Journal of Thoracic and Cardiovascular Surgery **F)** Graphic representation of the use of 3D printing to form microchannels *via* template micro-molding, permitting for the use of dynamic co-culture within a printed construct. [76] © 2014 Lab on chip
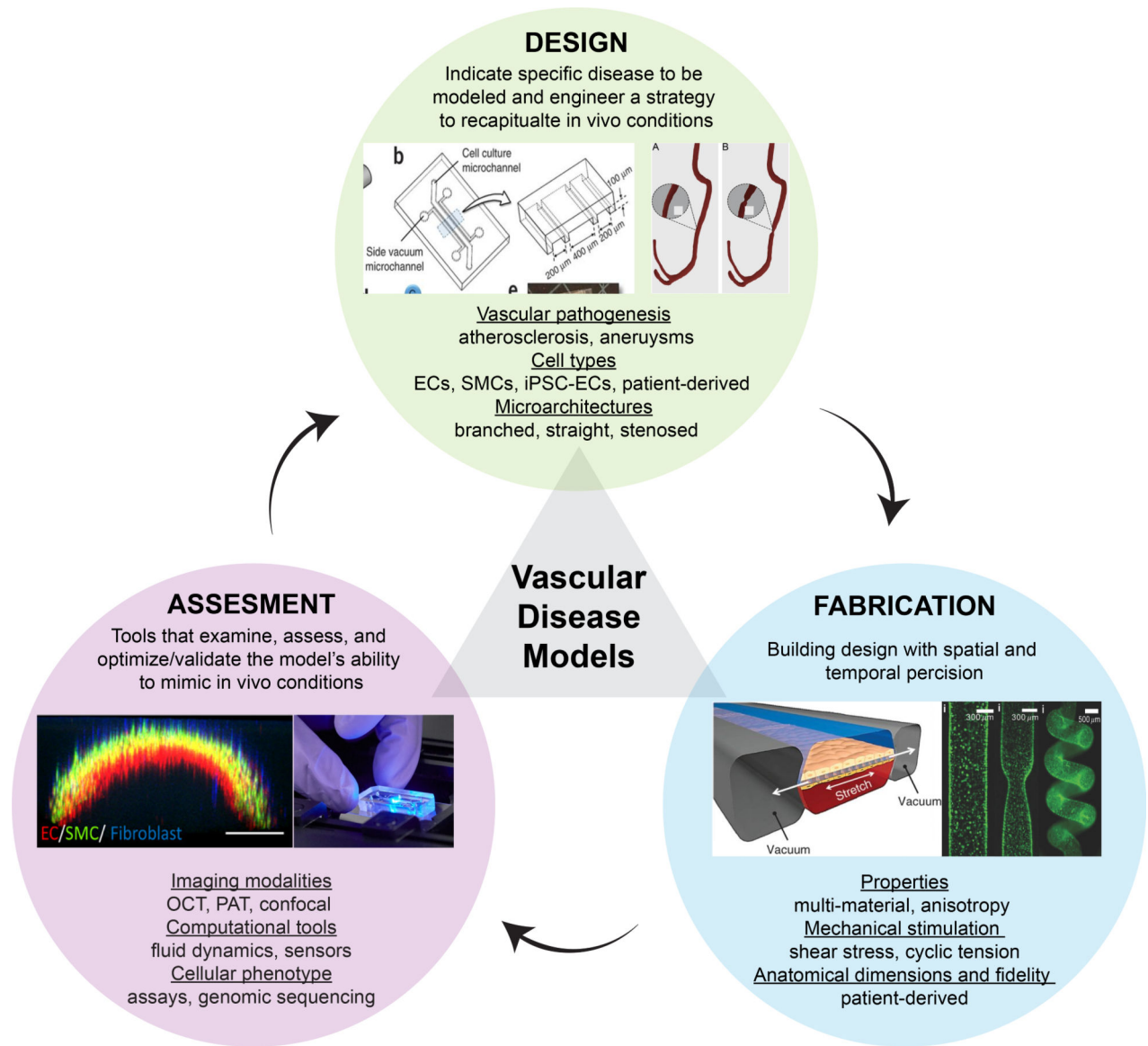
Figure 5:

The continuing cycle of model designs, fabrication techniques, and assessments/validations provides an engineered platform to mimic and test vascular physiology, functionalities, and response to drugs and toxins. [160] © 2013 Nature Protocols [161] © 2017 American Chemical Society [162] © 2018 Advanced Functional Materials [163]© 2015 Nature [157] © 2018 American Chemical Society

Table 1:

Advantages and Limitations of animal models of vascular diseases

	Rodent Models	Large Animal Models	Non-human Primates
Advantages	+ Ease of genetic manipulation, breeding, costs and time frame	+ Close to human anatomy (i.e. hear size and coronary circulation) + Close to human genetic composition (i.e. lipoprotein metabolism, enzymatic activity, cholesterol distribution) + Circulating volumes reflect similar volumes to humans + Increased tissue availability + Facilitates in collection of noninvasive measurements	+ Phylogenetically closest to humans (i.e. analogous diet, metabolism) + Develop vascular disease with age + Close to human genetic composition (i.e. lipoprotein metabolism, enzymatic activity, cholesterol distribution) + Increased tissue availability + Facilitates in collection of noninvasive measurements
Limitation	– Compromised lesion development – Varied anatomy – Increased heart rate – Diverse lipoprotein ranges – No expression of cholesteryl ester transfer protein – Inability and infrequency of plaque rupture and thrombosis	– Restrictions on genetic manipulations to mimic human physiology – Difficult to extrapolate, interpret, and relate data to humans – Difficult to isolate relevant tissues/cells for experimental response – Inability and infrequency of plaque rupture and thrombosis	– Significant restrictions due to ethical concerns – Threat to maintain biodiversity – Require long-term experimentation

Table 2:

Bioengineered vascular disease models using organ-on-a-chip technology

Material	Cell Type(s)	Blood flow conditions	Experiment	Ref.
PDMS	Mouse olfactory harvested arterial segments	Perfusion inlet was subjected to 45 mmHg and the outlet at atmospheric pressure.	Artery segments were reversibly loaded onto device; verified cellular arrangement of artery in chip by staining SMC nuclei, actin, and voltage gated calcium channels; vessel constriction was reduced by 50% after incubating with calcium-blocker nifedipine	Yasotharan et al.[68]
PDMS coated with VWF/ fibrinogen	HUVECs	Parallel microchannels with one-side stenosis of 20, 30, 40, 60, or 80 percent lumen reduction; human blood was perfused at 1,000 s^{-1} input wall shear rates	Stenotic chambers demonstrated enhanced platelet aggregation in 60 – 80% occlusion over a range of input wall shear rates; flow increases EC VWF secretion in stenotic outlet, causing platelet aggregation and post-stenotic thrombus formation	Westein et al.[74]
Gelatin-Agarose IPN	HUVECs, HDMVECs, HLMVECs	Physiologically relevant stiffness ~ 20 kPa (stiffness of healthy arteries between 1 and 35 kPa); Flow velocity in smallest channels set to ~2.8 mm s^{-1} (corresponding to a wall shear stress ~8.8 dynes cm^{-2})	Stiffer IPNs (~50 kPa) resulted in increased permeability compared to soft devices (~5 kPa); Extracellular haem (haemolytic by-product) induces delayed and reversible EC permeability (dose-dependent manner)	Qui et al.[164]
PDMS and collagen	hBMSCs, hFs, HUVECs, HASMCs	No profusion mentioned	Inflammatory factors (LPS, thrombin, and TNFα) compromises EC barrier function; Simultaneous inhibition of Rac1and activation of RhoA induced loss of HASMC exposure to HUVECs and reduced barrier function;	Alimperti et al. [165]

Material	Cell Type(s)	Blood flow conditions	Experiment	Ref.
			CRISPRmediated knockout of *N*-cadherin in HASMCs led to loss of barrier function and over expression in HUVECs *N*-cadherin (validated in mouse model)	
PDMS coated with collagen	HUVECs	Perfused human citrated whole blood at a flow rate of 0.29 mL min^{-1}, yielding a shear rate of ~1,000 s^{-1}	SLA printed miniaturized vascular structures that closely mimic stenotic and healthy blood vessel architecture; 15 minutes of blood perfusion revealed induced thrombosis down stream and at the stenotic regions whereas healthy geometries showed no platelet adhesion	Costa et al.[161]
PDMS	Resistance arteries isolated from wile	Harvested arteries were fixed at periphery and subjected to external pressure of 45 mmHg	Developed a microfluidic platform to assess resistance artery structure and function; fully automated acquisition of up to ten does-response sequences of	Günther et al.[166]
	type CD1 mice or CD1 mice expressing Tie2-GFP transgene in ECs	above atmosphere (aligned artery); Disk of sapphire uniformly distributed heat generated by thermoelectric heater; Flow in channels between 0 – 4 mL h^{-1}	intact mouse mesenteric artery segments; Exposure of phenylephrine or acetylcholine yield dose-response relationship identical to human response	
PDMS	HUVECs, HMVEC	Citrated human blood was perfused to obtain a wall shear rate of 750 sec^{-1} (~10 dynes cm^{-2} stress); for plateletendothelial dynamics, higher wall shear rate was used (750 sec^{-1}; ~30 dynes cm^{-2} stress)	Performed quantitative analysis of organ-level contributions to inflammation-induced thrombosis; LPS endotoxin directly stimulates intravascular thrombosis by activated alveolar epithelium; analyzed inhibition of EC activation and	Jain et al.[167]

Material	Cell Type(s)	Blood flow conditions	Experiment	Ref.
			thrombosis due to PAR=1 antagonist	
Fibronectin crosslinked gelatin	iPSC, NRVMs	Bulk elastic modulus of ca 50 – 100 kPa; lower concentrations obtained modulus between 1 and 15 kPa	Micropatterned gelatin hydrogels using laser-etching to obtain surface grooves and pillar structures with a resolution of 15 μm; verified structural organization, contractile function, and long-term viability compared to manually patterned gelatin substrates	Janna et al.[168]
PDMS	HAECs and HASMCs	Vacuum side channels induce cyclic strain of 5 – 8% to mimic stretching and relaxation of the channels; flow in EC chamber produced a wall shear stress of 1 – 1.5 PA	Culture of SMCs and EC with a porous membrane separating the two chambers lead to prolonged viability of cells that exhibited physiological morphology and organization through cell-cell contact;	Engeland et al.[169]

Abbreviations: IPN, inter-penetrating network; HUVECs, human umbilical vein endothelial cells; HDMVECs, human dermal microvascular endothelial cells; HDMVECs, human lung microvascular endothelial cells; PDMS, poly(dimethylsiloxane); hBMSCs, human bone marrow stromal cells; hFs, human lung fibroblasts; HASMCs, human aortic smooth muscle cells; LPS, lipopolysaccharides; HMVEC, human lung microvascular endothelial cells; PAR-1, protease activated receptor-1; iPSC, induced pluripotent stem cells derived cardiomyocytes; NRVMs, neonatal rat ventricular myocytes.

Table 3:

Bioengineered vascular disease models using 3D printing technology

Material	Cell Type(s)	Mechanical Conditions	Experimental Specifications	Ref.
GelMA for bulk material and Pluronic F-123 for sacrificial microchannels	HUVECs, hDFs	Reynolds number lower than 0.5 for flow rates between 0.6 and 3 mL h^{-1} (laminar flow); main velocities in main channel between 0.19 and 0.54 mm s^{-1}; burst pressure: ~ 0.16 ± 0.08 kPa; Compression moduli varied between 0.8 kPa to 0.65 kPa	Sacrifical bioprinting produced hDF encapsulated in GelMA with microchannels (washed out pluronic) devices lined with a confluent layer of HUVECs; profusion of blood formed thrombi that was exposed to tissue plasmin activator and subsequent dissolution of nonfibrotic clots; hDF were able to migrate into the clot and deposited collagen over time	Zhang et al.[75]
Nanosilicates, GelMA, kappacarrageenan	MC 3T3 Preosteoblasts	Addition of nanosilicates to the network induces a Herschel-Bulkley fluidic behavior, promoting a shear thinning profile with a power law index of 0.55	Utilized a ionic and covalent network stabilized by nanosilicates to produce high fidelity printed constructs; performed rheological modeling to determine optimal parameters for printing	Chimene et al.[114]
PEGDA, Alginate	PAVIC	Alginate was incorporated into bioink to increase precursor viscosity to permit for printing of high fidelity constructs; Lower weight percent of bioink had increased linear elasticity behavior, higher weight percent bioink exhibited nonlinear tensile stress-strain behavior	3D printing and photo-crosslinking technique to construct heterogeneous aortic valve to mimic the anatomic and axisymmetric geometries	Hockaday et al.[115]
Alginate, Collagen	Mouse fibroblasts, mouse SMCs, and HUVECs	Construct exhibited a linear stress-strain profile with an ultimate strength increases with increasing alginate concentration (0.049 MPa to 0.139 MPa); After 5 days of culture, the ultimate tensile strength decreased further to 0.105 MPa	3D printing of multi-level fluidic channels deposited in a layer fashion to replicate the hollow, lamellar vascular structure; demonstrated modeling potential using mechanical and chemical stimulation with a circulation flow system, an arterial surgery simulator, and cell coculture	Gao et al.[112]
Bioink: Fibrin composites Sacrificial ink: Gelatin, glycerol, and hyaluronic acid	CM	Printed at 18C with a pneumatic pressure of 100 kPa and a speed of 100 mm/min; intrinsic force generated within printed construct was 1.5 mN	3D bioprinted organized and functional cardiac tissue; printed constructs elicited physiological responses to cardiac drugs to alter beating frequency and contractility forces	Wang et al.[137]
PGA-co-PLCL	Obtained through implantation	Burst pressure: 11,685 ± 11,506 mmHg (postimplant), 6,167 ± 5,627 mmHg (preoperative); Compliance: 4.0% ± 1.5% (preoperative), 2.3% ± 0.46% (post-implant)	Created a patient-specific nanofiber vascular graft combining electrospinning and 3D Printing; implanted in sheep, demonstrating no aneurysm formation or ectopic calcification; explanation revealed complete resorption of grafts, SMC organization, ECM deposition,	Fukunishi et al.[153]

Material	Cell Type(s)	Mechanical Conditions	Experimental Specifications	Ref.
			endothelialization, and and similar mechanical properties to native vasculature	
PEGDA and GelMA	HUVECs, NIH/3T3 Fibroblasts	Viscous bioink (Reynolds number ~ 10 – 100) permits for smooth transitions between bioinks; Printing resolution ~ 20 – 30 µm	Stereolithography-based, multimaterial bioprinting platform for heterogeneous hydrogel constructs; Constructs loaded with VEGF were assessed for its neovascularization potential	Amir et al.[101]
GelMA and agarose	HepG2/C3A cells (encapsulated); HUVECs (seeded)	Youngs modulus of GelMA ~ 12.1 ± 1.1 kPa; pore size of GelMA ~ 143.2 ± 6.4 µm; perfusion was conducted at 50 µL h^{-1}	Sacrificial bioprinting technique produced hollow microchannels; HUVEC layer delayed permeability of biomolecules and showed increased viability of HEPG2/C3A cells	Massa et al.[102]

Abbreviations: HUVECs, human umbilical vein endothelial cells; PEGDA, poly(ethylene glycol) diacrylate; GelMA, Gelatin Methacrylol; VEGF, vascular endothelial growth factor; hDFs, human dermal fibroblasts; hMSCs, human mesenchymal stem cells; CM, cardiomyocytes; PGA, polyglycolic acid; PLCL, poly(L-lactide-co-ɛ-caprolactone); PAVIC, porcine aortic valve interstitial cells

Table 4:

Material properties of human vasculature and common vessel models.

Materials	Maximum Stress (MPa)	Maximum Strain	Elastic modulus (MPa)	Notes	Ref.
Healthy coronary artery	1.44 ± 0.87	0.54 ± 0.25	1.48 ± 0.24	Average age 38.07 ± 8.58; Strain rate of 1 mm/min	Karimi et al. [6]
Diseased coronary artery	2.08 ± 0.86	0.35 ± 0.11	3.77 ± 0.38	Average age 65.50 ± 10.33; Strain rate of 1 mm/min	Karimi et al. [6]
Layer-specific mechanical properties of coronary arteries	Adventitia: 1.43 ± 0.604 (circumferential) 1.3 ± 0.692 (longitudinal) Media: 0.446 ± 0.194 (circumferential) 0.419 ± 0.188 (longitudinal) Intima: 0.394 ± 0.223 (circumferential) 0.391 ± 0.144 (longitudinal)	Adventitia: 1.66 ± 0.24 (circumferential) 1.87 ± 0.38 (longitudinal) Media: 1.81 ± 0.37 (circumferential) 1.74 ± 0.28 (longitudinal) Intima: 1.6 ± 0.29 (circumferential) 1.55 ± 0.40 (longitudinal)	n.m.	Average age: 71.5 ± 7.3 years old	Holzapfel et al. [170]
Inferior vena cava	n.m.	n.m.	n.m.	Burst Pressure (mm Hg): 13,062 ± 6,847 Compliance: 2.4% ± 0.85%	Fukunishi et al. [153]
Elastin/Collagen	0.5017 ± 0.3665	0.2855 ± 0.1210	Elastin: 0.49 ± 0.18 Collagen: 131 ± 64	Monfrel dogs aged 54.9 ± 8.8 months weighing at 20.4 ± 1.8 kg	Armentano et al. [171]
PDMS	5.39 ± 1.23	144 ± 9.3			Jang et al. [172]
PDMS	n.m.	n.m.	0.005 − 1.72	Increasing elastic moduli demonstrates higher surface roughness; Strain ranged from 0 − 10 %	Palchesko et al. [173]
PDMS	n.m.	n.m.	2.04 ± 0.06 (10:1 PDMS:crosslinker) 0.42 ± 0.05 (30:1 PDMS:crosslinker)	0.1 N load with 0.01 mm displacement resolution; 10% strain applied to each sample at a rate of 0.25 mm s^{-1}	Carrillo et al. [174]
GelMA, κCA, & nSi (NICE)	0.3017 ± 0.021	70%	Tension: 0.495 ± 0.150 Compression: 0.0711 ± 0.0049	Demonstrated > 75% recovery after cyclic deformation	Chimene et al. [114]
GelMA	n.m.	n.m.	0.0005 − 0.001	Strain rate of 0.2 mm min^{-1}	Zhang et al. [75]

Materials	Maximum Stress (MPa)	Maximum Strain	Elastic modulus (MPa)	Notes	Ref.
GelMA	n.m.	n.m.	0.0121 ± 0.0011	Tried to mimic vascularized liver (elastic modulus: 0.0055 ± 0.0016 MPa)	Massa et al. [102]
Sodium Alginate	0.049 ± 0.005 (2 wt.%) to 0.184 ± 0.008 (4 wt.%)	1.53 ± 0.10 (2 wt.%) to 1.97 ± 0.009 (4 wt.%)		Ramp force with a slope of 0.5 N min^{-1}	Gao et al. [112]
PEGDA (700 MW:8000 MW)	n.m.	20 wt.% PEGDA 700: 0.50 ± 0.15 10 wt.% PEGDA 8000: 1.6 ± 0.1	0.0053 ± 0.0009 (20 wt.% PEGDA 700) to 0.0746 ± 0.0015 (10 wt.% PEGDA 8000)	Loaded quasi-statically at 0.02 mm s^{-1} until failure with strain rate of 0.005 s^{-1}	Hockaday et al. [115]
PGA and PLCL	n.m.	n.m.	n.m.	Burst Pressure (mmHg): $6{,}167 \pm 5{,}627$ (pre-operative) $13{,}062 \pm 6{,}847$ (6-months postoperative) Compliance: $4.0\% \pm 1.5\%$ (preoperative) $2.3\% \pm 0.46\%$ (postoperative)	Fukunishi et al. [153]
PLLA and SPEU-PHD	90/10 Outer-layer with 50/50 Innerlayer PLLA/PHD: 2.07 ± 0.17 (circumferential) 2.56 ± 0.28 (axial)	90/10 Outer-layer with 50/50 Innerlayer PLLA/PHD: 233.17 ± 34.62 (circumferential) 142.14 ± 23.87 (axial)	PLLA: 13.85 ± 3.82; 90/10 PLLA/PHD: 6.30 ± 0.75 50/50 PLLA/PHD: 5.35 ± 0.98 PHS: 0.56 ± 0.27; 90/10 Outer-layer with 50/50 Innerlayer PLLA/PHD: 6.24 ± 1.69 (circumferential) 29.54 ± 5.85 (axial)	Suture retention and burst pressure was dependent on thickness	Montini-Ballarin et al. [175]

Abbreviations: n.a., not measured; PDMS, Polydimethylsiloxane; GelMA, Gelatin Methacrylate; κCA, κ-carrageenan; nSi, Nanosilicates; NICE, nanoengineered ionic-covalent entanglements; PEGDA, Poly(ethylene glycol) diacrylate; PGA, Polyglycolic acid; PLCL, Poly(L-lactide-co-ε-caprolactone); PLLA, Poly(L-lactic acid); SPEU-PHD, pigmented poly(ester urethane)-PHD